NMR IN BIOMEDICINE
NMR Biomed. 2004;**17**:240–262
Published online in Wiley InterScience (www.interscience.wiley.com). DOI:10.1002/nbm.900

Review Article

Assessment of tumor oxygenation by electron paramagnetic resonance: principles and applications

Bernard Gallez,* Christine Baudelet and Bénédicte F. Jordan

Biomedical Magnetic Resonance Unit and Laboratory of Medicinal Chemistry and Radiopharmacy, Université Catholique de Louvain, Brussels, Belgium

Received 25 March 2004; Accepted 5 May 2004

ABSTRACT: This review paper attempts to provide an overview of the principles and techniques that are often termed electron paramagnetic resonance (EPR) oximetry. The paper discusses the potential of such methods and illustrates they have been successfully applied to measure oxygen tension, an essential parameter of the tumor microenvironment. To help the reader understand the motivation for carrying out these measurements, the importance of tumor hypoxia is first discussed: the basic issues of why a tumor is hypoxic, why these hypoxic microenvironments promote processes driving malignant progression and why hypoxia dramatically influences the response of tumors to cytotoxic treatments will be explained. The different methods that have been used to estimate the oxygenation in tumors will be reviewed. To introduce the basics of EPR oximetry, the specificity of *in vivo* EPR will be discussed by comparing this technique with NMR and MRI. The different types of paramagnetic oxygen sensors will be presented, as well as the methods for recording the information (EPR spectroscopy, EPR imaging, dynamic nuclear polarization). Several applications of EPR for characterizing tumor oxygenation will be illustrated, with a special emphasis on pharmacological interventions that modulate the tumor microenvironment. Finally, the challenges for transposing the method into the clinic will also be discussed.

KEYWORDS: EPR; ESR; NMR; *in vivo*; PEDRI; oxygen; tumor; cancer; spectroscopy; imaging; nitric oxide; irradiation; dynamic nuclear polarization; OMRI

INTRODUCTION

The aim of this manuscript is to provide an overview of the principles and techniques that are often termed EPR oximetry, to discuss the potential of such methods, and to illustrate how these methods have been successfully applied to characterize oxygen tension, an essential parameter of the tumor microenvironment. The importance of tumor hypoxia is first reviewed: the basic issues of why a tumor is hypoxic, why these hypoxic microenvironments promote processes driving malignant progression, and why hypoxia dramatically influences the response of tumors to cytotoxic treatments. More traditional methods and other methods under development for estimating tumor oxygenation will be briefly reviewed. To introduce the basis of EPR oximetry, the specificity of *in vivo* EPR will be discussed by comparing this technique with NMR. The different types of paramagnetic oxygen sensors will be presented, as well as the methods for recording the information (EPR spectroscopy, EPR imaging, dynamic nuclear polarization). Several EPR applications for characterizing the tumor oxygenation will be illustrated. Finally, the challenges for transposing the method into the clinic will also be discussed.

**Correspondence to:* B. Gallez, CMFA/REMA, Avenue Mounier 73.40, 1200 Brussels, Belgium.
E-mail: Gallez@cmfa.ucl.ac.be
Contract/grant sponsors: Belgian National Fund for Scientific Research; Fonds Joseph Maisin; 'Actions de Recherches Concertées'; NCI; *contract/grant number:* PO1EB002180.

Abbreviations used: CB, carbon black; CW, continuous wave; dHb, deoxyhemoglobin; DNP, dynamic nuclear polarization; EPR, electron paramagnetic resonance; HFB, hexafluorobenzene; LiPc, lithium phthalocyanine; NIRS, near-infrared spectroscopy; PFC, perfluorocarbon; PC, paramagnetic centers; SI, signal intensity; VEGF, vascular endothelial growth factor.

TUMOR HYPOXIA: THE CAUSES

Hypoxia has been known for a long time to be an important physiological parameter in tumor growth and response to therapy. Mechanistically, tumor hypoxia results from an imbalance between oxygen delivery and oxygen consumption[1] (Fig. 1). On the one hand, the oxygen delivery is impaired by structural abnormalities present in the tumor vasculature.[2,3] These include caliber variations with dilated and narrowed single branches of tumor vessels, non-hierarchical vascular networks, disturbed precapillary architecture, and incomplete vascular walls. These structural abnormalities cause numerous functional impairments, i.e. increased transcapillary permeability,[4,5] increased vascular permeability,[6] interstitial hypertension, and increased flow resistance. On the other

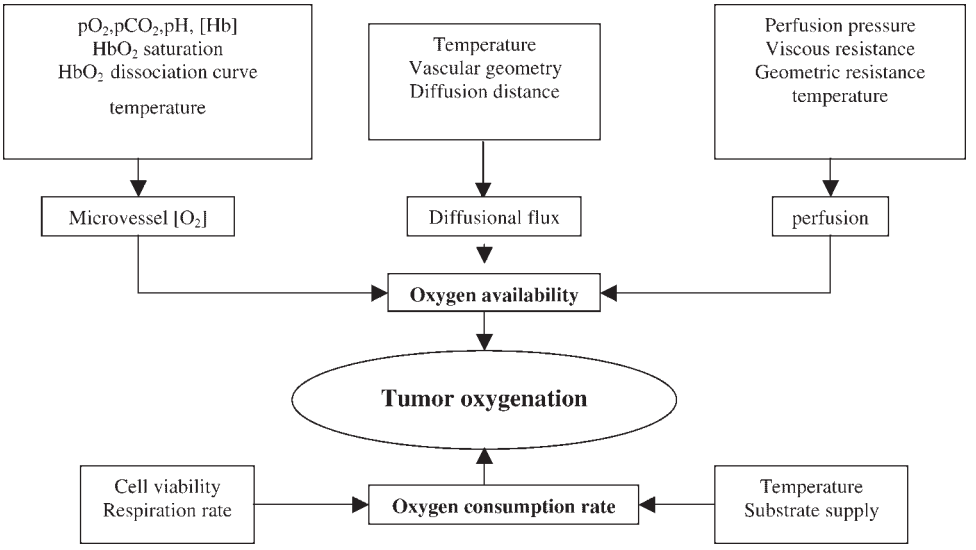

Figure 1. Factors responsible for the modulation of tumor oxygenation. (adapted from Vaupel *et al.*[1])

hand, the altered tumor cell metabolism with elevated metabolic rates also contributes to the occurrence of hypoxic regions in tumors. It is generally believed that tumor hypoxia develops in two ways: chronic hypoxia (or diffusion-limited hypoxia) and acute hypoxia (or perfusion-limited or fluctuating hypoxia).

Chronic hypoxia has classically been thought to result from long diffusion distances between tumor vessels as the consequence of the more rapid expansion of tumors cells than of supporting vasculature.[7,8] It is now well established that steep longitudinal gradients of pO_2 along the vascular tree, as opposed to radial diffusion of oxygen, can largely contribute to deficiencies in tumor oxygen supply.[9] Two features of longitudinal gradients lead to intravascular hypoxia. First, the arterioles feeding the tumor are more deoxygenated than comparable arterioles of normal tissues. The relative deoxygenation of these arterioles is probably due to tumor acidic pH, which leads to a right shift of the hemoglobin saturation curve. The second cause of exaggerated longitudinal gradients is the relative lack of arteriolar supply. Additionally, intravascular hypoxia may be responsible for altered blood viscosity, which could contribute to sluggish flow that is often found in tumors. Another important feature is the irregular geometry of vascular networks. Secomb *et al.* developed a scenario where there is adequate vascular density, but the chaotic nature of the vascular geometry creates hypoxia.[10] Abnormal branching angles lead to situations where vessels carry plasma but no red blood cells.

The origin of tumor *acute hypoxia* is not firmly established.[11] The commonly held view has been that acute hypoxia results primarily from vascular stasis, which stems from one of three causes: (1) vascular collapse in regions of high tumor interstitial pressure; (2) vessel plugging by leukocyte; or (3) impingement of tumor cells on the vascular lumen. The incidence of the total vascular stasis is low (5%), as measured using matched dye methods or intravital microscopy.[12,13] This has led researchers to believe that total vascular stasis is not likely to be a major cause for transient hypoxia in tumors. On the contrary, flow instabilities turn out to be a rather common phenomenon. Trotter *et al.* performed a series of studies in murine tumors using pairs of fluorescent dyes. They noted differences in staining intensity around groups of vessels and hypothesized that this may be due to fluctuations in blood flow within small networks of vessels.[14] Using laser-Doppler technology, temporal variations in perfusion have been seen in both experimental and human tumors.[15–17] Kimura *et al.* demonstrated that temporal instability in tumor red blood cell flux could lead to transient hypoxia.[18] Dewhirst *et al.* linked temporal changes in microvessel red blood cell flux with changes in the oxygen content in the same vessel.[13] Factors that may contribute to flow fluctuations include arteriolar vasomotion,[13,19] rapid vascular modeling,[20] and other hemodynamic effects such as nonlinear flow properties of blood, non-uniform axial distribution of red blood cells within the vessel, or disproportionate cell partitioning at bifurcations.[21] In addition, a model has recently been developed to explain the oscillatory behavior of tumor blood flow observed *in vivo*. It has been shown that, in the presence of moderate leakiness, the fluid dynamics of tumor circulation evolves toward a sustained oscillatory response, both in the microvascular pressure and blood flow.[22]

TUMOR HYPOXIA: THE CONSEQUENCES

Experimental and clinical evidence suggest that the hypoxic fraction in solid tumors may: (1) promote

metastasis; (2) select cells with a malignant phenotype; (3) promote angiogenesis; and (4) reduce the sensitivity of tumors to various treatment modalities.

Tumor hypoxia promotes metastasis

Several experimental models have shown that tumor hypoxia is associated with an increased ability to form metastases.[23] Young and co-workers demonstrated many years ago that murine tumor cells exposed to severe hypoxia increased their metastatic potential.[24] The causal link between hypoxia and metastasis was later demonstrated *in vivo*. Hypoxia is able to promote tumor metastasis in two ways: (1) by inducing the expression of gene products involved in the metastatic cascade; and (2) by providing selection pressure for a more aggressive phenotype. The initiation of metastasis is a multiple pathway that involves three major processes: degradation of the basement membrane and extracellular matrix, modulation of cell adhesion molecules and cell migration. The effects of low pO_2 on metastasis are correlated to expression of vascular endothelial growth factor (VEGF).[25] Low pO_2 increases metastasis whether the cells are treated *in vitro* prior to injection[24] or the whole animal is exposed to transient hypoxia.[26]

Tumor hypoxia selects cells with a more malignant phenotype

Hypoxia provides a physiological selective pressure in tumors for the expansion of variants that have lost their apoptotic potential, and in particular for cells acquiring p53 mutation.[27] The selective pressure resulting from hypoxia is not limited to the selection of cells with reduced apoptotic potential. It has also been shown to provide a possible selection force for cells that have altered oncogenic pathways that result in a switch to a more angiogenic phenotype. By promoting the clonal expansion of cells with reduced apoptosis and increased angiogenesis, hypoxia can contribute to the development and malignancy of tumors. Clinical results showing that hypoxic cervical cancers with low apoptotic index are highly aggressive support this basic experimental concept.[28]

Tumor hypoxia promotes angiogenesis

Tumor progression requires the formation of new blood vessels in order to provide nutrients and remove catabolites from the expanding tumor mass. Angiogenesis is also essential for the efficient dissemination of primary tumor cells during metastasis. The early steps of angiogenesis in tumors are nearly identical, as both processes involve degradation of the extracellular matrix and directed migration of either vascular or neoplastic cells. In addition, angiogenesis requires proliferation of the migrating endothelial cells. Initiation of angiogenesis begins when cells within the tumor microenvironment respond to hypoxia by the production of VEGF.[29] In addition to VEGF, hypoxia is also responsible for inducing the expression of the VEGF receptors (VEGFR1 and VEGFR2) through HIF-1 mediated transcription. Thus it would seem that hypoxia efficiently promotes an angiogenic signal by regulating both the VEGF ligand and its receptors.

Changes in gene expression that accompany tumor hypoxia

The multiple roles assigned to hypoxia, including the induction of angiogenesis, apoptosis and metastasis, probably result in large part from changes in gene expression that accompany hypoxia. A significant number and wide variety of hypoxia-induced genes have been described, including oncogenes, tumor-suppressor genes, stress proteins and cytokines. Cells exposed to hypoxia upregulate the expression of several transcription factors. Perhaps the most important within this group is HIF-1, which induces the expression of more than 30 known genes,[30,31] essential for energy metabolism (i.e. glucose transporters GLUT1 and GLUT3), iron metabolism (i.e. transferring and its receptor), hormone regulation (i.e. erythropoietin) and vasoreactivity (i.e. endothelin-1, nitric oxide synthase, VEGF).

Tumor hypoxia increases the resistance to radiotherapy

Traditionally, tumor hypoxia is considered to be a therapeutic problem, as it makes solid tumors resistant to ionizing radiation and some forms of chemotherapy.[32] Tumor hypoxia causes severe problems for radiation therapy (X- and γ-radiation), because the radiosensitivity is progressively limited when the pO_2 is below 10 mmHg. Hypoxia-associated resistance to photon radiotherapy is multifactorial. The presence of molecular oxygen increases DNA damage through the formation of oxygen free radicals, which occurs primarily after the interaction of radiation with intracellular water.[33] Because of this so-called 'oxygen enhancement effect', the radiation dose required to achieve the same biologic effect is about three times higher in the absence of oxygen than in the presence of normal levels of oxygen.[34,35] The critical value is about 5 mmHg. In a series of experimental and clinical studies, Vaupel and others showed definitively that measurements of pO_2 by polarographic microelectrodes provided useful criteria for predicting the response of tumors to radiation therapy.[36–42] According to Swartz,[43] these results are remarkable in two ways:

(1) the results demonstrate an immediate potential clinical use of methods developed to measure pO_2; and (2) the method used was productive even though it had significant limitations, including invasiveness and a resolution of the order of magnitude of the critical value, i.e. 5 mmHg. Therefore, he concluded that a more accurate, more facile method should provide even more useful data and could be applied more widely.[43]

Tumor hypoxia increases the resistance to chemotherapy

Cells located distant from a functional blood supply can be resistant to drug therapy because of several factors. First, a limited penetration of anti-cancer agents would result in lower efficacy. It has indeed been shown that the drug toxicity falls off as a function of distance from blood vessels.[44] Second, as a result of decline in nutrient and oxygen availability, cells further away from the vascular system would be dividing at a reduced rate and thus would be protected from the effects of chemotherapeutic agents whose activity is selective for rapidly dividing cell populations. The large difference in proliferation rate between cells located in perivascular areas and those adjacent to necrotic regions was first demonstrated by Tannock[45] and confirmed using the DNA-binding fluorochrome Hoechst 33342 by Olive.[46] Besides the inhibition of cell proliferation, multiple mechanisms are probably also involved in the hypoxia-induced resistance to chemotherapeutic agents, for example hypoxia-induced decreased cytotoxicity of certain agents,[44,47] and tissue acidosis. Furthermore, hypoxic stress proteins and the loss of apoptotic potential can impart resistance to certain chemotherapeutic drugs.[48–50] Finally, the resistance of solid tumors to chemotherapy may also be the result of another largely ignored perspective: that of tumor-specific fluctuations in blood flow. Fluctuating hypoxia has significant implications for delivery of chemotherapeutic agents, cellular responsiveness to those agents, and the regrowth potential of the surviving tumor cells. Moreover, regions actively proliferating at one point in time may not have cells actively synthesizing DNA at a different time.[51,52]

TECHNIQUES FOR THE ASSESSMENT OF TUMOR OXYGENATION

The assessment of tumor oxygenation may have profound therapeutic implications in oncology. Understanding of tumor hypoxia could lead to the discovery of diagnostic and prognostic markers for malignant progression, and identification of novel therapeutic targets. Hence, a non-invasive technique that could accurately and repetitively measure tumor oxygenation would find broad applications in clinical and basic research. The existing methods for directly measuring pO_2 in cells and tissues include magnetic resonance (MR)-based methods and non-magnetic resonance-based methods (Table 1). The advantages and disadvantages of the currently available methods will be briefly presented.

Table 1. Methods for measuring oxygen in tissues

MR-based methods	Non-MR-based methods
NMR	Polarographic oxygen electrodes
^{19}F relaxometry	Fluorescence quenching
BOLD effect	Phosphorescence quenching
EPR-related methods	Near-infrared spectroscopy
EPR	2-Nitroimidazoles
Dynamic nuclear polarization	

The non-MR-based oximetry methods include:

(1) *polarographic oxygen electrodes*—polarographic measurements of pO_2 depend on measurements of the current formed at a cathode upon ionization of oxygen at -0.7 V vs NHE (normal hydrogen electrode). All types of polarographic methods suffer from signal-to-noise problems at low oxygen tension because the pO_2 is directly proportional to the current generated at the cathode. The Eppendorf® electrode system has a computerized driver that moves the electrode through the tissue in a precise configuration that minimizes compression artifact on the tissue and consumption of oxygen by the electrode. It has been used as the 'gold standard' for measurement of tissue oxygenation.[53,54] The major problem of this technique is that it cannot make repeated measurements in the same position because it must be moved to minimize oxygen consumption by the electrode itself. Alternatively, recessed tip microelectrodes as compared with the Eppendorf® system, permit continuous recordings of tissue oxygenation without moving the probe. The degree of spatial resolution achievable is dependent on the effective size of the tip electrode. This type of electrode has been used in window chamber tumor preparations to measure oxygen gradients between tumor vessels,[55] perivascular oxygen concentrations of tumor venules and arterioles,[56] and transients in pO_2 occurring as a result of variations in red cell flux in individual microvessels.[18] The method has also been used to obtain temporal data on kinetics of pO_2 fluctuation for Fourier transform analysis of pO_2 fluctuations[17] and to monitor changes in pO_2 in response to drug treatment.[57,58]

(2) *fluorescence quenching*—an oxygen sensing method based on fluorescence quenching has been used in a commercial system that involves the insertion of a fiber-optic probe directly into the tissue. The system, with the brand name OxyLite®,

has a ruthenium complex-based fluorophore compound embedded in a rubber matrix at the tip of a 220 micrometer-diameter fiber-optic probe. Photodiodes (460 nm excitation blue light) stimulate the fluorophore, and the lifetime of the fluorescence is inversely proportional to the oxygen tension at the probe tip. The method is temperature-sensitive, thus quantification requires temperature correction, which is accomplished by thermocouples attached to the fiber-optic probes. The calibrations are stable and the sensitivity is highest at lower pO_2 values. The fiber optic oxygen sensor can be used to continuously monitor changes in pO_2 in a single spot.[59] Thus, the spatial distribution is limited to the number of probes inserted. Multiparameter monitoring is possible. The OxyLite system has been designed to operate in conjunction with OxyFlo (laser Doppler) for simultaneous monitoring of tissue pO_2 and blood flow from the same location. Some studies have compared the OxyLite system with polarographic electrodes.[60,61] Braun and co-workers found that OxyLite tends overestimate severely hypoxic fractions.[61] Increased pressure at the insertion of the probe may have contributed to low values measured with the OxyLite probe. Another explanation involves the sensing volume of the probe. Because the OxyLite averages over an area several hundred times larger than the microelectrode, it tends to smooth out some heterogeneity in the pO_2 distribution. The OxyLite systems have been used to measure pO_2 changes in experimental tumors following different interventions.[61–69] A limitation of the method is the impossibility to record pO_2 from the same site over days.

(3) *phosphorescence quenching*—phosphorescence lifetime imaging has been used to evaluate changes of oxygenation of tumors during procedures to manipulate tumor oxygenation. Using a multi-frequency phosphorimeter that collects data for many frequencies at the same time, it has been possible to determine oxygen distributions (oxygen histogram) using data collected in as little as 8 s.[70] The method is based on the oxygen-dependent quenching of phosphorescence emitted by albumin bound metal–porphyrin complexes after pulsed light excitation, in which the decay rate is directly related to the concentration of molecular oxygen.[71] The actual size of the sampled volume is dependent on the depth of light penetration into the tissue and consequently on the excitation wavelength. The development of phosphor compounds excited at long wavelength (636 nm) has made it possible to make phosphorescence measurements through a substantial (cm) thickness of tissue.[72]

(4) *near-infrared spectroscopy (NIRS)*—this technology can provide an efficient, real-time, non-invasive approach for monitoring tumor blood oxygenation dynamics of tumor.[73,74] In the near-infrared range (650–1000 nm), oxyhemoglobin (HbO_2), deoxyhemoglobin (dHb), and oxidized cytochrome oxidase have characteristic absorption spectra.[75] NIRS can be used as a continuous monitor of changes in blood oxygenation and blood volume by following changes in the concentrations of HbO_2 and the total hemoglobin concentration. This method does not provide a real tissue pO_2 measurement.

(5) *drugs which localize selectively in hypoxic tissues*—in 1976, Varghese *et al.* reported that ^{14}C-labelled misonidazole formed adducts in hypoxic cells *in vitro* and *in vivo*.[76] It was subsequently found that adducts form with thiol groups in proteins, peptides and amino acids in such a way that all atoms of the ring and side-chain of the 2-nitroimidazole are retained.[77,78] Hypoxia ($pO_2 <$ 10 mmHg) is required for binding, which suggests that bioreductive markers (2-nitroimidazole derivatives) can be used to detect hypoxic cells.[79–81] Bioreductive markers are selectively reduced only in *viable hypoxic* cells, so they have a theoretical advantage over polarography for determination of relevant hypoxia. Indeed, pO_2 electrodes show no discrimination of cell type or viability and thus will record readings from less significant (radiobiologically speaking) tissue. This may also explain why Eppendorf pO_2 values do not always correlate with the 2-nitroimidazole-based hypoxia marker studies. Moreover, detection of hypoxia marker binding is dependent on having hypoxia present for hours. Most investigators believe that binding of such agents to tumors reflects primarily diffusion-limited hypoxia.[82] A variety of non-invasive assays for tissue hypoxia based on 2-nitroimidazoles have been developed. Various labeled derivatives are PET active.[82–84] Alternatively, the immunohistochemical hypoxia technique is particularly attractive because gradients of hypoxia can be visualized and compared with underlying hierarchical structures in tissues and with gene expression on a cell by cell basis (such as blood perfusion, necrosis, proliferation, differentiation, apoptosis or oxygen-regulated protein expression).[85,86] The technique is based on monoclonal and polyclonal antibodies raised against protein adducts of reductively activated 2-nitroimidazoles. The intensity of binding of 2-nitroimidazoles in immunohistochemistry may not form a sufficient basis for distinguishing transient hypoxia from true steady-state diffusion limitation of oxygen. It should be emphasized that the binding depends not only on the pO_2, but also on the content of reductases and on the perfusion that may limit the accessibility of the nitroimidazole to the cells.

The MR-based methods to evaluate tissue/tumor oxygenation include NMR spectroscopy and imaging as well as EPR and related methods, such as dynamic nuclear polarization that combine aspects of EPR and NMR. Several NMR techniques have been developed that yield physiological information in addtion to high-resolution anatomical details. Both magnetic resonance imaging (MRI) and magnetic resonance spectroscopy (MRS) have provided unique insights into tumor vasculature and the interaction between vasculature, physiology and metabolism. An excellent review by Gillies *et al.* was recently published about the NMR view on the tumor microenvironment.[87] The indirect detection of oxygen by NMR can be performed by observing the effect of the paramagnetism of oxygen on NMR signals and the alteration of the relaxation times.[88] The effect of oxygen on NMR relation times is ubiquitous, but for tumor applications, ^{1}H and ^{19}F have mainly been used.

(1) *^{19}F NMR spectroscopy/imaging*—^{19}F NMR spectroscopy and imaging of perfluorocarbon (PFC) emulsions have been used extensively to measure oxygen tension in biological systems. The favorable biocompatibility of PFCs allows intravenous injection of these compounds in large doses. In tumors with leaky vasculature, PFC microdroplets can pass through the fenestrations in the vascular wall and accumulate in the interstitial space.[89] Macrophages do not seem to take up PFC[90] so that the pO_2 is mainly interstitial. In most ^{19}F NMR relaxometry studies PFCs are administered a few days before the MR measurement to allow the circulating PFCs to be sequestered in tumor tissue. Oxygen-sensitive ^{19}F NMR relies on the fact that the NMR spin-lattice relaxation rate R_1 $(1/T_1)$ of the PFC is enhanced in direct proportion to the dissolved O_2 concentration.[91] Local oxygen tensions are derived from T_1 relaxation rates. However, PFC spin–lattice relaxation rates may also depend on other physiological or histological parameters. For example, tumor temperature is an important factor to control because the T_1 relaxation time of ^{19}F spins is also related to tissue temperature. A number of PFCs have been surveyed and hexafluorobenzene (HFB) has been identified as the best pO_2 reporter. Symmetry provides a single narrow ^{19}F NMR signal and the R_1 is highly sensitive to changes in pO_2, yet minimally responsive to temperature.[92] It is also well characterized in terms of lack of toxicity. Intratumoral injection of PFCs compared with i.v. administration is an attractive alternative to assess tissue pO_2 in the hypoxic region.[93] The recently developed 'fluorocarbon relaxometry using echo planar imaging for dynamic oxygen mapping' technique (FREDOM), which includes intratumoral injection of HFB, has increasingly been appreciated because pO_2 distribution assessed with the Eppendorf histograph is in agreement with FREDOM.[94,95] Using FREDOM, repeated quantitative maps of regional pO_2 can be achieved and changes in tumor pO_2 can be monitored (e.g. in response to carbogen).[96] Alternatively, fluorinated nitroimidazoles have also been used to detect tumor pO_2. MR-visible derivatives have been produced that retain their visibility even after sequestration. These include Ro07-0741, CCI-103F and SR-4554, which remain NMR-visible even after nitroreductive bioactivation.[97] SR 4554 shows higher retention in hypoxic tumor, but the correlation between retention of ^{19}F signal and pO_2 was not straightforward.

(2) *BOLD imaging*—the blood oxygen level-dependent (BOLD) contrast mechanism in brain was first described by Ogawa *et al.*[98,99] in rat studies using NMR at strong magnetic fields (7 and 8.4 T). Ogawa noticed that the contrast of very high resolution images acquired with a gradient-echo pulse sequence depicts anatomical details of the brain as numerous dark lines of varying thickness. By accentuating the susceptibility effect of dHb in the venous blood with gradient-echo techniques, he discovered that image contrast reflected the blood oxygen level. As is now known, the phenomenon is indeed due to the field inhomogeneities induced by the endogenous MRI contrast agent dHb. In dHb, the iron (Fe^{2+}) is in a paramagnetic high spin state (d^4) as four out of six outer electrons are unpaired. The paramagnetic nature of dHb can modify the strength of the magnetic field passing through it. It enhances the R_2 $(=1/T_2)$ and $R_2^*(=1/T_2^*)$ transverse relaxation rates of water in blood and in the tissue surrounding the blood vessels. In the simplest model, these relaxation rates change linearly with deoxyhemoglobin concentration, which therefore acts as an endogenous contrast agent for blood oxygenation. Apart from its very large application in neuroscience, the use of BOLD contrast in tumor brings with it new challenges of understanding and interpretation.[100] The underlying physiological changes are different from those of BOLD in the brain. In the brain, blood vessel size, density and distribution are well characterized, in contrast to tumors. The assumptions used in models to describe BOLD contrast of fMRI in brain cannot therefore be applied to tumors. Gradient echo imaging, which provides BOLD contrast, has been used to investigate parameters related to tumor vasculature, such as perfusion, blood oxygenation, blood vessel development, remodeling and function, as well as to monitor the effects of therapy changing the tumor oxygenation. BOLD contrast changes were also recently detected in rodent tumors with high spectral and spatial resolution (HiSS) MRI rather than with conventional GRE imaging.[101] The sensitivity of BOLD contrast techniques to changes in tumor

dHb concentration is of relevance to many strategies in cancer treatments, particularly with regard to interventions designed to alter tumor oxygenation. One vascular intervention currently being assessed for its ability to improve tumor oxygenation prior to radiotherapy is carbogen (95% CO_2/5%O_2) breathing and nicotinamide in combination.[102] Increases in tumor GRE (gradient recalled echo) image intensity have been reported during carbogen breathing and during hyperoxia.[63,65,103–110] The main cause of the GRE image intensity change is the increase in blood oxygenation through the breathing of a high-oxygen-content gas, reducing the dHb concentration of tumor blood vessels. The increased blood oxygenation associated with carbogen breathing produces a decrease in $R_2^*(=1/T_2^*)$. Similarly, a decrease in the dHb content of the tissue will also occur if there is an increase in blood flow, since the fraction of oxygen extracted from the blood is reduced. Additionally, the GRE image intensity at a short repetition time will be T_1-dependent and changes in blood flow can change the apparent T_1 via the 'in-flow effect'. To emphasize the importance of flow effects, the term FLOOD (flow and oxygenation dependent contrast) has been used.[111,112] Alternatively, multi-gradient echo imaging sequences can be used to enable absolute R_2^* relaxation rates to be calculated, independent of the inflow effect.[113] Changes in R_2^* in response to a vasoactive challenge are not always predictable.[100] An R_2^* decrease is expected in response to agents aimed at improving tumor oxygenation and blood flow, and conversely an increase in R_2^* is expected with agents designed to increase tumor hypoxia. However, changes in blood volume can counteract the effect of blood oxygenation changes. Moreover, changes in blood pH and glucose levels can alter oxygen extraction. The relationship between GRE MRI response and tumor pO_2, the critical parameter with respect to treatment outcome, was investigated by invasive Eppendorf histography during carbogen breathing.[111] An apparent lack of correlation between BOLD MRI and pO_2 histography was observed. However, Al Hallaq *et al.* observed a strong correlation between water resonance linewidth decrease and O_2 microelectrode data during carbogen breathing averaged over the whole tumor.[114] The questions that remained were: in view of tumor heterogeneity, how good was the correlation between the MR parameters in gradient-echo imaging (signal intensity, SI) or effective transverse relaxation time (T_2^*) and local partial pressure of oxygen (pO_2)? Was the magnitude of the change in SI or T_2^* a quantitative marker for variation in pO_2? To address these questions, murine tumors were imaged during respiratory challenge using fiber-optic microprobes to simultaneously acquire tumor pO_2 and erythrocyte flux.[65] In each tumor, the BOLD signal response (SI and T_2^*) was temporally correlated with changes in pO_2. However, the magnitude of the signal bore no absolute relation to pO_2 across the tumors. For example, a given change in SI corresponded to a 25 mmHg pO_2 change in one tumor, but to a 100 mmHg change in another.[65] Moreover, the initial T_2^* value did not reliably predict tumor oxygenation. Information afforded by the BOLD imaging technique is therefore qualitative in nature. If an absolute measurement of pO_2 is needed, it should be combined with another technique capable of providing an absolute measurement of pO_2. The major advantages of the BOLD-related techniques applied to tumors include non-invasiveness, high spatial resolution, and real-time detection of fluctuations. The real-time evolution of changes in oxygenation and/or perfusion can be mapped, and the tumor heterogeneity response can be taken into account using convenient statistic tools.[115] Moreover, recent studies described the usefulness of BOLD imaging to produce maps of spontaneous fluctuations of flow/oxygenation (tumor acute hypoxia) in experimental tumors.[116,117]

The other MR-based methods include EPR oximetry and related methods such as dynamic nuclear polarization. This is the subject of the rest of this paper. Since EPR is less 'popular' than NMR, we will first compare both techniques to show complementarity and specificity of EPR. After that, we will describe the principles of measuring oxygen using EPR.

COMPARISON BETWEEN NMR AND EPR: SPECIFIC PROBLEMS OF *IN VIVO* EPR SPECTROSCOPY AND IMAGING

EPR (electron paramagnetic resonance) or equivalently ESR (electron spin resonance) is a magnetic resonance method that detects only species containing unpaired electrons. Although there are few fundamental differences between the principles of electron and nuclear magnetic resonance, differences in physical and chemical properties of the resonant species (unpaired electrons vs nuclei with net spin) lead to profound differences in the techniques that are used to record the spectra. Three major differences can be emphasized: the ratio between the frequency and the magnetic field, the need for paramagnetic compounds and the very short relaxation times observed for the electron spins.

Frequency/magnetic field ratio

The greatest difference between NMR and EPR arises because the gyromagnetic ratio of an unpaired electron is 659 times larger than that of a proton, so the resonance

frequency/magnetic field ratio for the electron is 28 GHz/T, vs 42.5 MHz/T for the proton. Consequently, standard EPR spectrometers operate at much higher frequencies and lower fields than conventional NMR spectrometers. While EPR spectroscopy now is performed using a wide range of frequencies, from radio frequencies to infrared, most standard commercial spectrometers operate at 9.5 GHz (X-Band) for a magnetic field of about 0.34 T. At this frequency, non-resonant absorption of the electromagnetic radiation by the liquid water of the biological samples presents a serious problem, thus limiting the sample size to a thickness of less than 1 mm. Several interesting studies analyzing the pharmacokinetics of paramagnetic compounds were obtained in mice by putting the tail of the animals directly in the EPR resonator.[118,119] As the tail veins of mice are superficial, a non-invasive monitoring of the concentration of paramagnetic compounds was achievable with high sensitivity and short time resolution between sampling. Larger aqueous samples or animals can be studied only by reducing the operating frequency to 1 GHz or less, but this results in a reduced sensitivity. At 1 GHz, the depth of sensitivity is about 1 cm, which is ideal for studies in rodents.[120,121] So far, most studies have been carried out at this frequency. The use of lower frequencies (300 MHz) would extend the sensitive depth to sampling volumes comparable to NMR studies.[122,123]

Paramagnetic materials

The lack of sufficient amounts of naturally occurring paramagnetic materials is another problem. Both calculations and direct observations have shown that endogenous paramagnetic species such as paramagnetic metal ions and free radicals are present in insufficient amounts to be detected directly by EPR *in vivo*. The short half-life of most free radicals is another source of difficulty in the study of paramagnetic species. Therefore, the paramagnetic substance has to be introduced as a probe into the system, which can cause problems with sensitivity and toxicity. On the other hand, using paramagnetic probes have some beneficial aspects, since the only paramagnetic species observed *in vivo* are those introduced by the experimenter. The absence of background signals is particularly convenient for *in vivo* EPR spectroscopy. With the addition of appropriate paramagnetic species, the sensitivity of EPR on a molar basis is about 700 times greater than for NMR. Identifying paramagnetic species that are very stable and have appropriate line shapes has been a significant factor in the successful development of *in vivo* EPR techniques.

Short relaxation times

The short relaxation times of most paramagnetic species can cause additional problems. The time scale of electron spin relaxation of most paramagnetic species is nanoseconds, in contrast to NMR where the relaxation times typically are milliseconds.[124] This has two major consequences. First, *in vivo* EPR spectra are mostly obtained through continuous wave (CW) experiments.[125] Instead of applying a pulse of radiowave energy and waiting for the transient response (as in clinical MRI), the sample is continuously irradiated with low-intensity electromagnetic radiation. The resonant response of the unpaired electrons is then measured by slowly increasing the strength of the applied magnetic field.[126] Most EPR studies have not been able to utilize the pulse techniques developed for NMR in biological systems. Only recently has significant progress been made in addressing the challenges of time-domain radiofrequency EPR.[127–129] The second consequence of short EPR relaxation times is that EPR imaging requires magnetic gradients that are at least one order of magnitude greater than those used in MRI. Additional problems for EPR imaging arise from the fact that EPR spectra for most paramagnetic species have multiple lines and multiple lineshapes. These spectral features, however, can be very valuable for EPR spectroscopy because they can provide very sensitive parameters of the environment (pH, microviscosity, etc.) in which the paramagnetic species are located.[130–133]

The key technical advances that were necessary to develop *in vivo* applications of EPR were: (1) instrumental development of spectrometers operating at low frequency (typically between 200 MHz and 1.5 GHz) suitable for use with animals; (2) development of detectors suitable for *in vivo* studies; (3) identification and development of paramagnetic compounds with properties suited for particular application (especially for the measurement of pO_2); and (4) improved methods for data acquisition and analysis.

PRINCIPLES OF EPR OXIMETRY

Physical interactions of molecular oxygen with paramagnetic species

Molecular oxygen is a triplet radical that possesses two unpaired electrons, which are responsible for its paramagnetism. In the gas phase, at very low oxygen partial pressure (i.e. 0.1 mmHg), it is possible to record an EPR spectrum with conventional EPR spectrometers.[134] However, no EPR spectra have been reported from oxygen dissolved in fluids near room temperature. There seems to be no possibility for the *direct* detection of oxygen in biological systems. The lines are so broadened as to be undetectable.

However, indirect methods exist. Most of these methods rely on the paramagnetic properties of molecular oxygen, which acts as an efficient relaxer for other paramagnetic species. Bimolecular collisions between

oxygen and free radicals alter the resonance characteristics of the radical and consequently the EPR spectrum. The enhancement of relaxation rates scales linearly with the concentration of oxygen over a wide range of oxygen tensions. Measurements that depend on T_1 and T_2 of EPR spin probes can provide a direct indication of the concentration of oxygen.[135,136] The most common method is to use the broadening of the principal hyperfine line (related to T_2). The line broadening is caused by Heisenberg exchange between molecular oxygen dissolved in solution and the radical.

For *soluble paramagnetic materials*, there is a direct relationship between the EPR line exchange broadening and the radical-radical collision rate.[135] The exchange rate ω is governed by the Smoluchowski equation:

$$\omega = 4\pi R\{D(O_2) + D(SL)\}[O_2]$$

and the variation of the EPR linewidth ΔLW is

$$\Delta LW = 4\pi Rkp\{D(O_2) + D(SL)\}(\Delta[O_2])$$

where R is the interaction distance, k is a proportionality constant, p is the probability that exchange will occur upon each collision, $D(O_2)$ and $D(SL)$ are the diffusion constants of oxygen and the spin label, respectively, and $[O_2]$ is the concentration of oxygen in solution.

For *particulate paramagnetic materials*, the relationship between the linewidth and the partial pressure of oxygen is more complex. Most particulate materials identified so far share an extremely large broadening per unit of pO_2, exceeding that of soluble radicals by several orders of magnitude. The interaction with oxygen responsible for the line broadening depends on the structure of the particulate material. For lithium phthalocyanine, the oxygen sensitivity is critically dependent on the crystal form. Oxygen has been shown to migrate in the channels presented by the tetragonal x-form and dramatically influence the magnetic behavior.[136–138] In carbonaceous materials (chars, coals, carbon blacks), the carbon-centered free radicals are stabilized over large aromatic ring clusters.[139] The mechanism of oxygen response has been studied in several synthesized chars. The results suggest that these compounds contain two types of paramagnetic centers (PC),[140,141] differing by their distance to the adsorbed oxygen molecules. Each type of PC is characterized by its own oxygen sensitivity and EPR linewidth. At low oxygen concentration, the extremely narrow EPR linewidth is the result of intensive Heisenberg electron–electron spin exchange between the radicals themselves. With increasing oxygen concentration, the paramagnetic oxygen molecules start to break up the radical–radical exchange, which leads to EPR line broadening. When the oxygen exceeds 3 mM, the two-dimensional dipole–dipole interactions between the paramagnetic centers come into play, and results in a change in broadening as well as in changes in EPR lineshape.[141]

In practice, a given paramagnetic material (soluble radicals or particulates) can be calibrated in terms of the effect of oxygen on the linewidth (Fig. 2). When introduced in a biological medium, the measurement of the linewidth of the probe can be directly interpreted in terms of the oxygenation in the vicinity of the probe (Fig. 3).

Types of spin probes

The lack of detectable levels of endogenous paramagnetic species makes it necessary to use exogenous paramagnetic materials. Not all paramagnetic substances are convenient for oximetry purposes. The main requirements in a paramagnetic probe suitable for oximetric applications are: a few narrow EPR lines, a good stability in the biological media, and no toxicity. As already stated, two classes of stable paramagnetic materials are useful for oximetry purposes: soluble paramagnetic materials and insoluble particulate materials.[142]

Soluble paramagnetic materials

Among soluble paramagnetic materials, two types of structures are particularly interesting: the nitroxides and the triaryl methyl radicals (Fig. 4). Nitroxides are free radicals where the unpaired electron is delocalized between nitrogen and oxygen. The steric hindrance around the nitroxide group is responsible for the stability of these compounds. A number of different properties of nitroxides can be manipulated. For example, a charged nitroxide will not cross the plasma membrane and thus can be used to measure the concentration of oxygen in the extracellular compartment; a neutral nitroxide will be distributed throughout the intracellular and extracellular environments.[143] Moreover, nitroxides can be linked to carrier molecules to achieve a tissue or organ selectivity.[144,145] The effect of oxygen on the linewidths of these compounds is fairly modest but may be sufficient for several applications. When the concentration of oxygen increases from 0 to 210 μM (the concentration of oxygen in a physiological solution in equilibrium with air), the EPR linewidth increases by approximately 100 mGauss. For most nitroxides, the linewidth in the absence of oxygen is approximately 1 Gauss. To increase the sensitivity to oxygen, it is convenient to use perdeuterated nitroxides,[119,135] for which the linewidth is lower than 200 mGauss. It is also possible to use nitroxides with a resolved superhyperfine structure to increase sensitivity to oxygen.[146] This method is only valid at low pO_2 because, at high concentration of oxygen, the superhyperfine structure is not resolvable. Another option is to encapsulate nitroxides in lipophilic environments. As oxygen is more soluble in organic solvents than in water, an increase in sensitivity has been demonstrated using these systems.[147] Nitroxides were also the first compounds that were tested in dynamic nuclear polarization

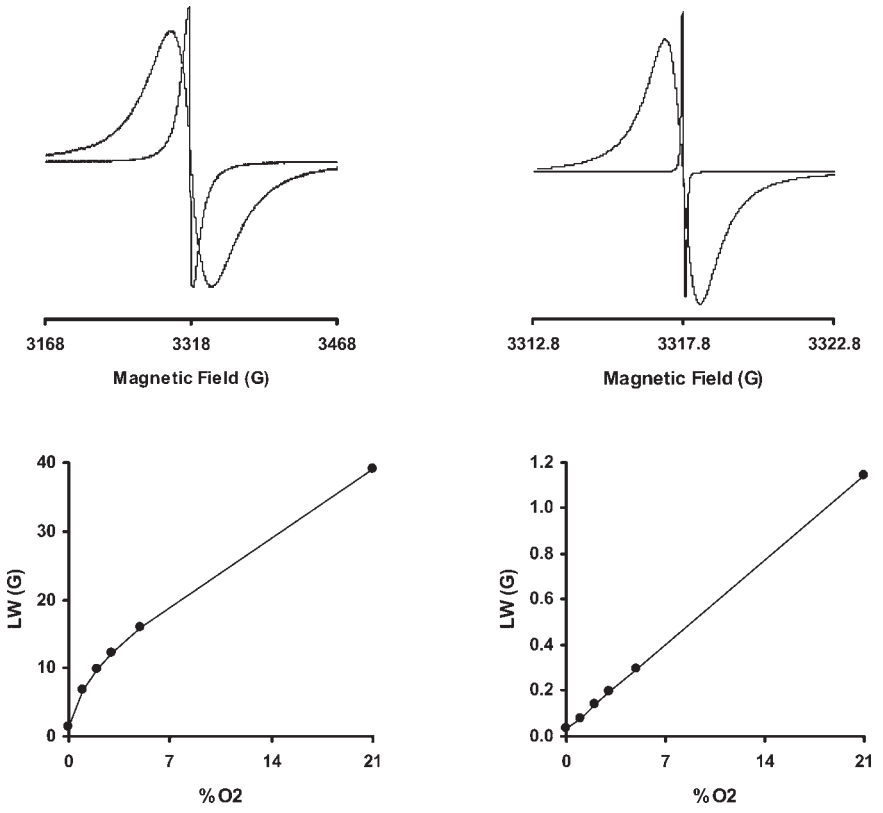

Figure 2. Effect of oxygen on the EPR spectra of paramagnetic particulate materials. Left: carbon black Printex U. Right: lithium phthalocyanine. Top: EPR spectra recorded in nitrogen (dark lines) or in air (21% oxygen) (gray lines). Bottom: calibration curve (linewidth as a function of the pO_2). Note the linearity of the response for the lithium phthalocyanine while the charcoal possess a curvilinear response, with a higher sensitivity to oxygen at low pO_2. Note also the order of magnitude of difference in terms of the linewidths observed when comparing both materials (300 Gauss sweep for the carbon black, 10 Gauss sweep for the Lithium phthalocyanine)

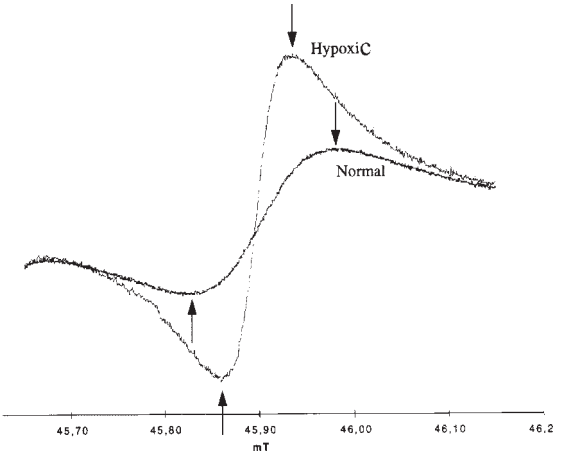

Figure 3. EPR spectrum of charcoal particles injected in the gastrocnemius muscle of a mouse in normal conditions or after a transient interruption of the blood flow. This spectrum was recorded using a low-frequency EPR spectrometer (1.2 GHz)

to probe the oxygen environment.[148,149] Nitroxides have the limitation of being metabolically converted to diamagnetic hydroxylamines. However, the bioreduction is dependent on the redox state of the tissues.[150–153] The kinetics are more rapid in strongly reducing systems, such as highly hypoxic tissues. This feature can be utilized to produce information on the redox state *in vitro* and *in vivo*. A study presenting the non-invasive imaging of tumor redox status was published recently.[154,155] Special care should be taken when linking the signal decay of nitroxides to the redox state, because the kinetics of clearance also depend on the perfusion (and wash-out from the tissue) and on the viability of cells.[119]

The recent development of triarylmethyl radicals (Fig. 4) has significantly expanded the potential for using oxygen-sensitive free radicals in EPR,[156–158] EPR imaging[128,159,160] and related techniques such as dynamic nuclear polarization.[161–163] In human blood, the stability of triarylmethyl radicals varies from a half-life of a few hours to one of more than 24 h depending on the particular structure of the compound. These compounds were first developed by Nycomed innovation. General

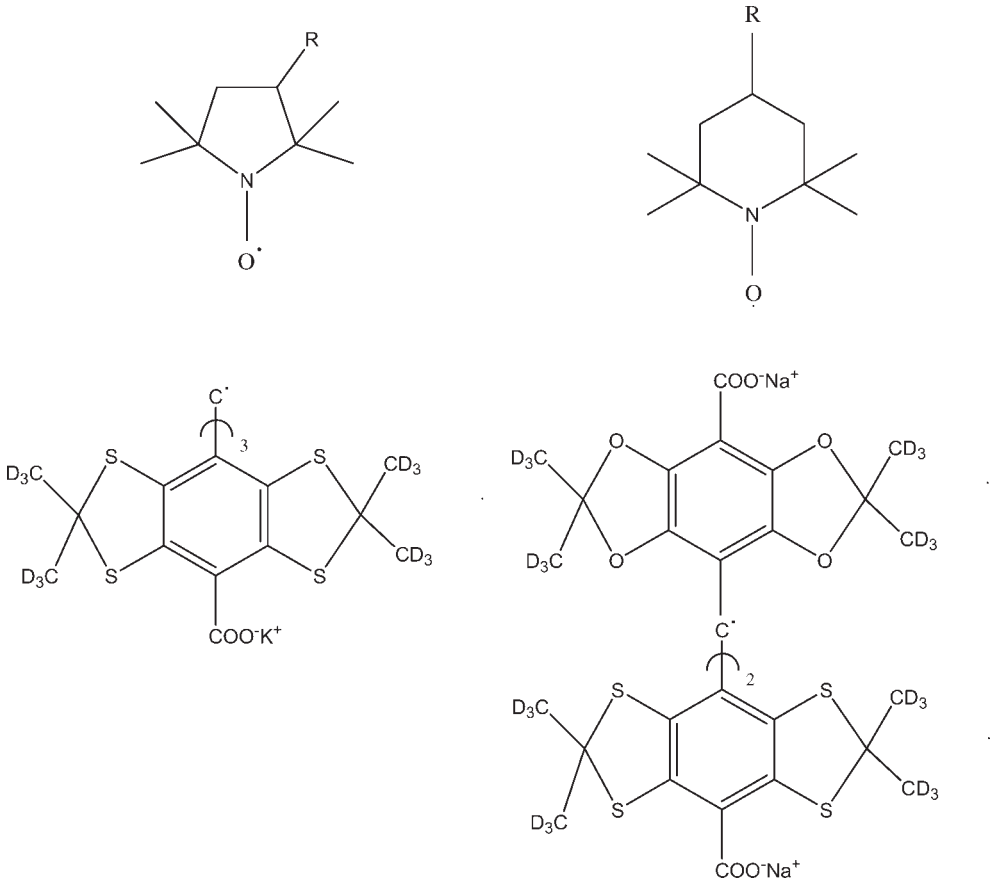

Figure 4. Chemical structures of stable soluble free radicals. Top: nitroxides; top left: pyrrolidine structures; top right: piperidine structures. Bottom: triarymethyl or trityl radicals; bottom left: example of symmetric trityl; bottom right: example of asymmetric trityl

synthesis of these types of products was also recently described.[164] The EPR spectrum of these compounds displays one single line with very small ^{13}C satellite lines.[156] One important interesting characteristic of triarylmethyl radicals is the narrowness of their EPR linewidth (typically less than 100 mGauss). As the signal intensity is inversely proportional to the square of the EPR linewidth, the sensitivity of detection is particularly convenient for *in vivo* applications using these compounds, especially for imaging studies. The EPR linewidth is linearly dependent on the concentration of oxygen.[156]

Particulate paramagnetic materials

The recognition of the potential value of oxygen-sensitive particulate paramagnetic materials has had a very strong impact on the development of EPR oximetry.[43,165,166] These substances all exhibit very strong, nearly Lorentzian lineshapes that broaden reproducibly in the presence of oxygen. These materials have several characteristics that are not shared by soluble free radicals. They can have high spin density combined with much larger sensitivity (up to 1000 × that of soluble materials) to oxygen, in terms of the magnitude of the change in line width per unit of oxygen. These materials also tend to be unreactive: they remain stable despite the presence of oxidation, large changes in pH and presence of other paramagnetic materials. A big advantage of these materials is their capability of providing repeated, sensitive, and accurate measurements of pO_2 at the same site. This is particularly useful for observing changes in pO_2 induced by physiological modulations or by pharmacological agents. There are several types of these materials with overlapping properties and characteristics: lithium phthalocyanine, lithium naphthalocyanine, coals, chars, inks and carbon blacks.

Lithium phthalocyanine. Lithium phthalocyanine (LiPc) is a crystalline material that is produced under very specific conditions. This material has an extremely narrow line of around 25–30 mGauss under 0% oxygen; this linewidth broadens proportionally to pO_2 with a linewidth of about 1000 mGauss in air.[167] The linearity of the response (Fig. 2) is especially valuable for measuring dramatic changes in pO_2: the signal-to-noise ratio is particularly high at low pO_2 due to the narrowness of the linewidth, and the linewidth at high pO_2 remains sufficiently narrow to get a reasonable signal to noise ratio in

these conditions. This feature permits the use of LiPc as an oximetry probe in brain.[168–170] The narrowness of the linewidth is also particularly suitable for multisite spectroscopy. One limitation of this material is the rapid saturation at low power. There are number of derivatives that have been developed: methyl and methoxy derivatives,[138] and lithium naphthalocyanine.[171] The latter is less sensitive to power saturation.

Coals. The initial studies used fusinite, a coal maceral which is insoluble, amorphous, aromatic, and of organic origin.[172,173] This coal is produced from materials which have burned before becoming fossilized. It is especially useful for measurements from 0 to 20 mmHg. At higher pO_2, the response is too small to provide accurate indications of the pO_2. A major problem is the availability of reproducible batches of fusinite having comparable EPR characteristics. Another coal, 'gloxy', has been found and characterized.[174] It has a smaller linewidth in the absence of oxygen, and a higher number of spins. Charcoals do not all have paramagnetic centers and, when they do, sensitivity to oxygen and stability *in vivo* are not always compatible with usefulness for *in vivo* EPR oximetry. In a large screening of analytical grade charcoals, two coals were identified that had considerable stability and sensitivity for oximetry purposes.[175] Like other charcoals, these materials have a very large sensitivity to changes in pO_2 at low pO_2. Such characteristics are particularly suitable for monitoring changes in pO_2 in tumors.[176] Typical EPR spectra recorded *in vivo* in hypoxia or normoxia are presented in Fig. 3. Several kilograms of these materials were characterized. Since one EPR oximetry study consumes only a few milligrams, hundreds of thousands of experiments can be carried out with this highly sensitive material.

Chars. Besides natural charcoals, the carbonization resulting from the heating of carbonaceous materials under an inert atmosphere induces solid graphite-like paramagnetic carbon materials.[139] While any organic material can be charred, the most useful materials appear to be those derived from carbohydrates and woody plants.[140,173] The controlled production of these materials is very complex because the response of the paramagnetic centers to pO_2 is extremely sensitive to the conditions under which the charring takes place.[140,177,178] On the other hand, this has some beneficial aspects. For example, the range of sensitivity can be adapted to specific needs such as high sensitivity at low pO_2 or modest sensitivity over a very large range of pO_2. One of the key issues for the applicability of these materials is overcoming the problem of the stability of the response to pO_2 in tissues.[179,180]

Inks and carbon blacks. Another type of particulate material that is particularly interesting for EPR oximetry can be found in India inks,[181,182] which are suspensions of carbon black (CB) particles. The first EPR oximetry experiments in humans were actually carried out using these inks.[181] These experiments raised great hope for immediate application of India ink as an oxygen sensor for clinical use, since these inks were already used for tattoos and surgery markings. Unfortunately, the EPR characteristics of these first inks were not optimal (low density of spins, multi-component signal). This stimulated a considerable amount of research that was carried out by ourselves and Swartz's group to identify new sensors among commercially available materials. Some interesting compounds were identified. However, it turned out that EPR properties varied from one batch to another within the same trademark. In order to isolate pure oxygen-sensitive carbon blacks and to achieve a long-term availability of oxygen sensors, a large screening on these types of materials was recently carried out. These experiments demonstrated that, within the 43 CBs analyzed, two compounds (Printex U and Printex 140 from Degussa-Hüls) had the most interesting EPR properties, including a high sensitivity of the linewidth to the changes in pO_2 (Fig. 2).[183] The sensitivity to oxygen is very large at low pO_2 (75 mT/mmHg), about 750 times more sensitive than soluble nitroxides. This sensitivity is very interesting for monitoring changes in pO_2 in tumors,[183] but the large EPR linewidth recorded at pO_2 above 15 mmHg and consequent low signal-to-noise ratio impedes its use in other normal tissues. Using these materials, it is now possible to manufacture inks stabilized in biocompatible dispersing agents.

PRINCIPLES OF DETECTION

Spectroscopy and multisite spectroscopy

The use of spectroscopy offers the advantage of maximum sensitivity. For this purpose, the particulate materials can be introduced into the tissue. Thus, the method is only invasive the first time. After that, the measurements can be made non-invasively using a surface coil.[120] This method is particularly well adapted for measurements of pO_2 from the same site over long periods of time, and offers the highest sensitivity in terms of pO_2. Variations in pO_2 of less than 1 mmHg can be detected using particulate materials. Of course, the spatial resolution is limited to the immediate vicinity of the particulate. However, this problem can be solved using multisite spectroscopy with appropriate gradients.[184]

Imaging. While EPR spectroscopy provides an absorption profile corresponding to a discrete or a global measurement of paramagnetic materials in an entire object, EPR imaging techniques provide spatially resolved measurements of these materials. The spatial distribution of free radicals can be performed utilizing magnetic field gradients in a manner similar to that of

NMR imaging.[185–189] Excellent reviews on principles of CW-EPR imaging[190] and time domain RF FT-EPR imaging were published recently.[129] Spectral–spatial EPR imaging encodes both the spatial distribution of the spin probe and the spectral information, which allows mapping of molecular oxygen.[159,160,191–198] For this purpose, the use of soluble EPR materials such as trityl radicals is more convenient as they can diffuse in the whole tissue. Compared with one-site and multisite EPR spectroscopy, there is a significant gain in terms of spatial information. However, this costs in terms of sensitivity to oxygen, because the soluble radicals are several times less sensitive to oxygen changes in the environment. Moreover, there is a need for repeated injections of the oxygen sensitive probe when performing studies on dynamic changes in pO_2 after chronic treatments.

Principles of DNP oximetry

Dynamic nuclear polarization techniques or DNP are alternative methods to EPR for detecting and imaging free radicals in biological samples or animals. In the literature, synonyms used to talk about the same method are PEDRI for proton electron double resonance imaging,[199–201] or OMRI for Overhauser magnetic resonance imaging.[163,202] The principle is based on the Overhauser effect, and uses a combination of EPR and MRI. It involves collecting a proton NMR image while irradiating the EPR resonance signal from the free radical under study. A transfer of polarization from the electrons to protons can occur, resulting in an amplification or enhancement of the observed NMR signal.[203] PEDRI uses standard MRI sequences but requires the additional capability of irradiating the sample at the EPR frequency. The basic PEDRI sequence still suffers from the need for EPR irradiation, so it is implemented at low field and is limited for large samples. The use of field-cycled PEDRI overcomes this limitation.[204] The principle is to use an EPR irradiation at low field, meaning low frequency where RF heating is minimal. The field is then increased to a much higher value so that the NMR signals can be measured with improved signal-to-noise ratio, and therefore provide a good image quality. Using this technique, how is it possible to extract information on the oxygen environment? It was found that the Overhauser enhancement factor is dependent on the linewidth of the paramagnetic compound: it is inversely proportional to the level of oxygen.[205,206] By collecting several DNP images that vary in the level of RF powers, it is possible to extract the electron T_2, and by this way, the pO_2.[124,163] This principle was recently published by Krishna applied to measure oxygen in murine tumors.[163] An image is first obtained after injection of a trityl radical. The image intensity is enhanced by the concentration of the contrast agent, and in regions that are hypoxic. By extracting the T_2, an oxygen image can be produced.

APPLICATIONS OF EPR TO MEASURE TUMOR OXYGENATION

EPR oximetry provides a potentially very useful method to follow changes in the pO_2 under various physiological and pathophysiological conditions.[43] This technique has already been used in brain,[168–170] heart,[193,207–211] gastrointestinal tract,[194] skeletal muscle,[147,167,171–175,183] liver,[212–217] kidneys[218] and skin.[181,219,220] However, since oxygenation is of crucial importance in tumors to predict the outcome of a treatment, and since there is hope for manipulating local oxygenation to improve the efficacy of anti-cancer therapies, many efforts have been carried out to apply this technology for the characterization of tumor oxygenation. In several studies, measurements of tumor oxygenation using EPR have been carried out as a proof of principle in order to show that a specific method or a newly developed paramagnetic material was applicable for this purpose.[119,183,160,214,221,222] In other studies, EPR oximetry was compared with other methods that provide direct or indirect measurements of tumor oxygenation: comparison with polarographic electrodes,[163,223] the distribution of nitroimidazoles,[83] the BOLD effect in MRI,[107,159,224] and pO_2 recordings using OxyLite®.[66–68] More interestingly, the power of EPR oximetry to measure oxygen from the same site over long periods of time offers the possibility of developing novel approaches to modifying tumor oxygenation, and thus optimizing anti-cancer treatments.

Attempts to treat tumors by changing their microenvironment can be achieved using some contradictory approaches. On the one hand, it is reasonable to try to chronically decrease tumor oxygenation, perfusion and feeding by nutrients necessary to the tumor development. This is the object of vascular targeting and anti-angiogenic approaches. On the other hand, a transient increase in tumor oxygenation and perfusion may be beneficial if combined with radiotherapy or chemotherapy. The tumor oxygenation may be modified by changing the oxygen supply (change in Hb saturation, change in perfusion) or by changing the local oxygen consumption. Several illustrative examples will be presented.

Modulations of tumor oxygenation by modifying the inspired gas

One way to increase the tumor pO_2 is to breath enriched-oxygen gas. Generally, carbogen, a gas containing 95% oxygen and 5% CO_2, is preferred to pure oxygen to avoid the vasoconstrictive effects of oxygen. Breathing carbogen (possibly combined with nicotinamide administration) is now applied succesfully in the clinic together

with irradiation.[102] The increase in pO_2 in tumors induced by breathing carbogen was shown in several tumor lines using EPR spectroscopy,[107,176,183,224] EPR imaging[146,160,159] or PEDRI.[163] Oxygen images were obtained in tumors before and after breathing carbogen by the group at the NCI using dynamic nuclear polarization and the extraction of T_2 of trityl radicals.[163] This effect of carbogen on tumor pO_2 and on tumor regrowth delay is also particularly interesting as a positive control for comparing the efficacy of other types of treatments.[66–68]

Manipulation of tumor oxygenation by pharmacological interventions

It is often assumed that tumor vessels are unable to autoregulate. In this context, the changes in tumor blood flow should mainly be the result of modifications in blood flow in adjacent normal tissues and arterial blood pressure.[8] Therefore, the change in tumor blood flow caused by external factors is greatly influenced by the structural relationship between the tumor vascular beds and those of the surrounding normal tissues. When the vascular beds in the tumor and those in normal tissues are in parallel, the change in blood flow would be opposite, for the following reason: an increase in normal tissue blood flow due to vasodilation would shunt away the blood flow from the tumor to the normal tissue, resulting in a decrease in tumor blood flow (steal effect). Conversely, when the tumor blood flow is in series with the normal tissue blood flow, the changes would be similar because the blood that leaves the normal tissue vascular bed directly flows into the tumor. 'Series' and 'parallel' types may be mixed or combined in a tumor.[225] The change in blood flow could vary, depending on the relative contribution of the series and parallel types. Nevertheless, this concept has to be considered with caution as it is a simple theoretical model. In experimental tumors, several agents have been identified that can improve tumor perfusion or oxygenation. Vasoconstrictors, like angiotensin II, vasopressin, norepinephrine, and vasodilators, like angiotensin-converting enzyme inhibitors and calcium antagonists, were tested.[225–227] It was also clear that only a few compounds were characterized for their effect on tumor oxygenation, although the choice among vasoactive agents was very large.

Using EPR oximetry, a large screening experiment was carried out to evaluate the effect of 34 vasoactive agents in experimental tumor models,[176] with the hope of identifying new radiosensitizing agents. Compounds of the following classes were tested: angiotensin-converting enzyme inhibitors, calcium antagonists, alpha antagonists, potassium channel openers, beta-blockers, NO donors and peripheral vasoactive agents. Twenty-four compounds were efficient in significantly increasing the local pO_2 in a majority of tumors.[176] The results obtained with the NO donors were particularly interesting, since all compounds were able to increase the pO_2 from a radioresistant status to a radiosensitive status (Table 2).

Table 2. Effect of NO donors on the local pO_2 measured in TLT tumors (adapted from Gallez *et al.*[176])

Compound	Dose (mg/kg)	Tumor pre (mmHg)	Tumor post (mmHg)	Responsive tumors
Isosorbide dinitrate	0.2	2.25 ± 0.39	8.36 ± 0.41*	8/10
Nitroglycerin	0.3	1.00 ± 0.98	5.31 ± 0.52*	7/10
Sodium nitroprusside	0.05	2.16 ± 0.50	9.56 ± 0.35*	10/10
Molsidomine	40	1.92 ± 0.98	6.48 ± 0.54*	8/10

*Significant difference before and 30 min after the treatment (*t*-test): $p < 0.05$.

One of these compounds was further characterized: isosorbide dinitrate, which is classically used in the treatment of angina. When the treatment was applied in two different murine tumor models (TLT and FSAII), a rapid increase of pO_2 was observed.[67,107] This increase in pO_2 led to a significant improvement of the treatment by radiotherapy (Fig. 5).[67]

Another type of radiosensitizing treatment that was identified by means of *in vivo* EPR oximetry is insulin infusion, which turns out to be nitric oxide-mediated.[66] It is known that insulin can modulate the blood perfusion in muscles, and the starting hypothesis was that insulin could also affect the tumor oxygenation. It has indeed been found in two tumor models that insulin dramatically increases the tumor pO_2. This results in a radiosensitisation effect (Fig. 6).[66] However, contrary to the starting assumption, this effect on the pO_2 was not due to an increase in blood flow. In fact, the blood flow was even decreased after insulin infusion, as shown by dynamic contrast enhanced MRI.[66] The increase in pO_2 was due to a dramatic decrease of the oxygen consumption. By molecular biology techniques, it has been shown that this effect involves an activation of eNOS, a release of high levels of nitric oxide and an inhibition of the mitochondrial respiratory chain.[66]

To continue with examples involving a nitric oxide pathway, the effect of the stimulation of muscle by electric pulses (in order to mimic muscle exercise) was explored.[68] After this type of stimulation, a significant increase in pO_2 was observed in the tumor compared with unstimulated muscle. The effect was rather prolonged, and it was found that the rapid increase was due to a transient increase in blood flow, an effect that was relayed by a decrease in oxygen consumption (Fig. 7).[68] The decrease in oxygen consumption was measured *ex vivo* by high-frequency EPR using sealed tubes with a suspension of tumor cells mixed with a solution of perdeuterated nitroxide. Again, the therapeutic relevance of this type of treatment was demonstrated: the stimulation of a muscle that is the host of a tumor leads to a radiosensitization of this tumor.[68]

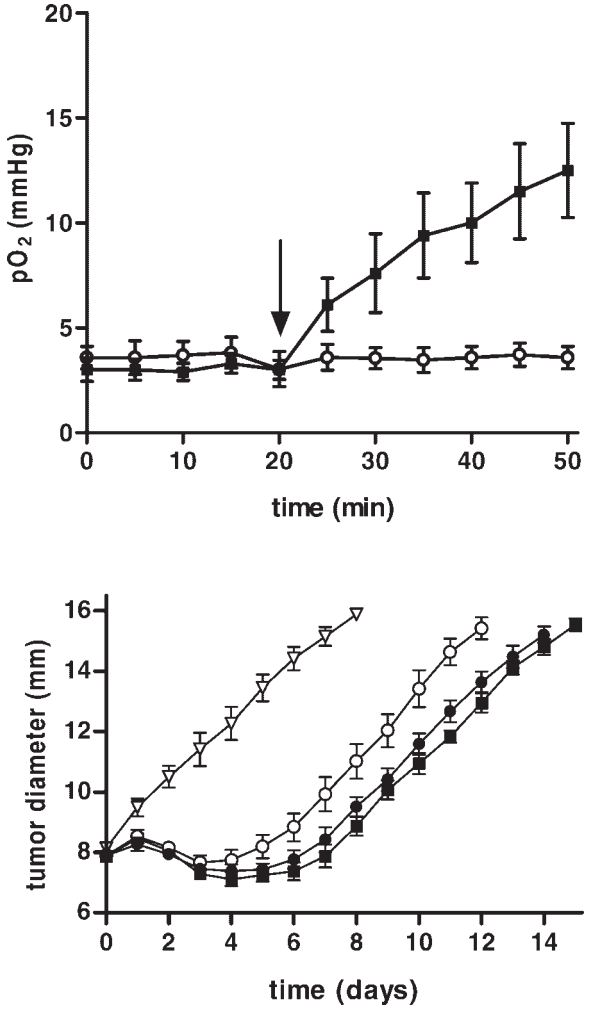

Figure 5. Effect of the administration of isosorbide dinitrate on tumor pO_2 and on sensitivity to irradiation. Top: effect of I.P. injection of isorsorbide dinitrate on the pO_2 in Fsall tumor as measured by EPR oximetry. The arrow indicates the administration of isosorbide dinitrate. Bottom: effect of the administration of isosorbide dinitrate on the tumor regrowth delay in the same tumor model. Triangle: control. Open circle: RX alone. Solid circle: RX + isorsorbide dinitrate. Square: RX + carbogen breathing. See Jordan *et al.*[67] for details

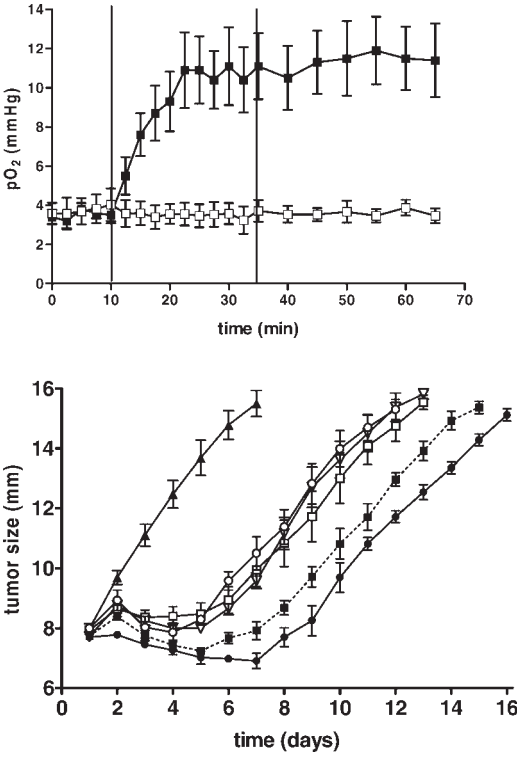

Figure 6. Effect of insulin infusion on tumor pO_2 and on sensitivity to irradiation. Top: effect of the injection of insulin on the pO_2 in FSall tumor as measured by EPR oximetry. Bottom: effect of the administration of insulin on the tumor regrowth delay in the same tumor model. Triangle: control. Open circle: RX alone. Solid circle: RX + insulin. Square: RX + carbogen breathing. Open triangle: RX + L-NAME. Open square: RX + insulin + pre-treatment with L-NAME. See Jordan *et al.*[66] for details. Note a larger effect for RX + insulin compared with RX + carbogen. Note also the abolition of the effect if L-NAME is administered prior to insulin

Strong support for the involvement of a nitric oxide pathway came from experiments carried out using $eNOS^{-/-}$ mice.[228] The increase in tumor oxygenation, as well the radiosensitizing effect, was abolished when using eNOS knock-out mice compared with wild type mice. Moreover, by a complete analysis of all nitric oxide-mediated treatments, it appeared that it was unlikely that oxygen alone was responsible for the radiosensitizing effect in specific conditions.[228] Using spin trapping studies that allowed the quantification of the release of nitric oxide in tumors, we showed that nitric oxide possesses an intrinsic radiosensitizing effect, additive to the effect on oxygen delivery and consumption.[228]

There are only a few examples so far that have used *in vivo* EPR oximetry in which the applied treatment leads to a reduction in tumor pO_2. Sersa *et al.* described the decrease of tumor oxygenation and blood flow after treatment with vinblastin[229] and after electrochemotherapy with cisplatin.[230]

Radiotherapy

Other examples of applications of EPR oximetry involve monitoring of tumor pO_2 induced by radiotherapy. It has been demonstrated in several tumor strains that 1 or 2 days after irradiation there is an increase of the tumor pO_2.[231–233] This provides additional motivation for fractionated irradiation and for monitoring pO_2 during irradiation treatment to determine the best window of opportunity for irradiating the tumor.[234] These pioneer studies were initiated by O'Hara and Swartz. The molecular basis of the increase in pO_2 was recently investigated in a study combining EPR oximetry and molecular biology: it turns out to be nitric oxide mediated by changes in expression of eNOS and caveolin.[235]

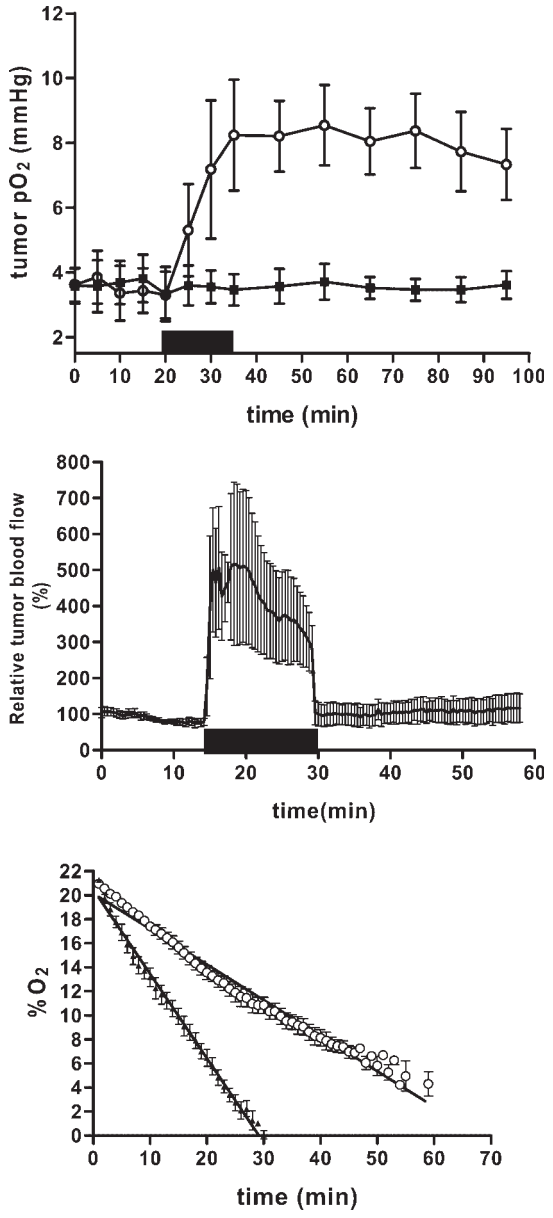

Figure 7. Effect of a muscle exercise protocol on the tumor pO_2 and contribution of flow and oxygen consumption to the modulation of the effect. Top: effect of exercise on the tumor pO_2 measured by *in vivo* EPR oximetry. The solid square indicates the period of stimulation of the muscle. Middle: effect on the tumor blood flow as measured by laser-Doppler implanted in the tumor. Note that the blood flow can explain the initial increase in pO_2, but cannot explain the delayed and remaining effect as the blood flow effect stopped when the stimulation protocol stopped. Bottom: effect on the oxygen consumption of tumor cells measured *ex vivo* by EPR oximetry. Note the decreased oxygen consumption for tumor cells in tumors implanted in a muscle that was then stimulated (circle), compared with the control tumor cells. See Jordan *et al.*[68] for details

Photodynamic therapy

Another example of the importance of timing when combining treatments is found in the field of photodynamic therapy. Pogue recently published results on the importance of the changes of pO_2 after photodynamic therapy using verteporfin as photosensitizer. He identified a time-window during which pO_2 increased significantly, and demonstrated that tumors were most sensitive to ionizing radiation in this time frame.[236,237]

Radioimmunotherapy

This last example illustrates the unique capability of EPR to repeat measurements of oxygen tension at the same site over long periods of time. Examining treatment outcome after radioimmunotherapy, O'Hara showed that the lowest response was observed in the tumors with the highest hypoxic fraction, while the responsive tumors were the ones which had the highest pO_2 when the treatment was initiated.[238]

FUTURE DIRECTIONS: TOWARD THE CLINIC?

EPR oximetry has become a routine method for measuring absolute pO_2 and variations at the same site over time. It has already opened up new avenues of investigation in fundamental research. It is very likely that the technology will expand, as several EPR companies are now manufacturing commercial low-frequency spectroscopy EPR and imaging systems for small animal research. The technology is therefore no longer limited to laboratories that are developing EPR technology.

Another very important question is how this powerful technology can be transposed into clinical practice in the future. Considering the unique information provided by this technology, this is certainly a valid goal. There are two major challenges for moving this technology into the clinic: (1) assuring biocompatibility of the oxygen sensors in humans; and (2) modifying the instruments so that they can be used for humans instead of small animals.

Biocompatibility of the oxygen sensors

The approval of oxygen sensors for use in human subjects depends on the approval of international or local regulators, such as the FDA in the USA or the EMEA in Europe. For soluble paramagnetic materials, the approval of trityl radicals will depend on the willingness of the pharmaceutical manufacturers to carry out the lengthy registration and approval procedures. So far, no toxic effects have been observed using these compounds in many experimental studies. For nitroxides, it is less clear that any particular company will push for its approval. However, little or no toxic effect has been recorded so far using these compounds.[239–243] For paramagnetic particulate materials, initial clinical

studies have already begun using India ink, which has been used in humans without toxicity for several centuries.[181,182] The first clinical trial, which was approved and begun at Dartmouth Medical School, will use India ink as an oxygen sensor. Another possibility for particulate materials is to encapsulate them in oxygen-permeable biocompatible polymers that are already approved for human use.[179,180,214,244–246]

Instrumental developments

The need for instrumental development was recently reviewed by Swartz, who developed the first clinical EPR facility.[247] Interestingly, whole body EPR systems have been built in the last few years in Hanover (USA), Columbus (USA), Chicago (USA) and Aberdeen (UK).[248,249] In addition, special coils (including implantable coils and catheter–resonators) have been developed. It appears that there is now ample opportunity for pioneering research using *in vivo* EPR in humans.

CONCLUSIONS

Magnetic resonance, especially *in vivo* EPR, is an emerging technology that has already proven very useful for the characterization of the tumor microenvironment. In addition to technological and electronic developments, efforts in developing oxygen sensors have been very successful. They can be used to characterize many physiological and pathophysiological systems. Using these sensors, it has been possible to explore better treatments for some therapeutic regimens of cancer therapy. Compared with other techniques, EPR oximetry has the advantage of being able to measure the absolute pO_2 with a minimal degree of invasiveness. One-site and multisite EPR spectroscopy provides maximum sensitivity to oxygen (variations of less then 1 mmHg can be measured), maximum speed (ability to make measurements in few seconds), and possible repeatibility of the measurement at the same site over long periods of time (several months if needed). EPR imaging or PEDRI using soluble materials that are able to diffuse into and within the area of interest extend the capability to three-dimensional measurements of oxygen tension, albeit with diminished sensitivity. Recent work has been carried out to develop sensors that could be used in the clinic for future studies. We believe that the efforts of the whole '*in vivo* EPR community' will be useful both for fundamental studies on the characterization of the tumor microenvironment and for the benefit of future cancer patients.

Acknowledgments

This paper was presented in part during the plenary session 'The tumor micro-environment' at the eleventh meeting of the International Society for Magnetic Resonance in Medicine, Toronto, July 10–16, 2003. Several leaders in the field contributed to this presentation by providing research materials from their groups: H.M. Swartz (Hanover, USA), M.C. Krishna (Bethesda, USA), D. Lurie (Aberdeen, UK), H. Halpern (Chicago, USA). They are acknowledged for their kind contribution. The work is supported by the Belgian National Fund for Scientific Research (FRSM, IISN, Televie), the Fonds Joseph Maisin, the 'Actions de Recherches Concertées', and the NCI (grant PO1EB002180). The authors would like to thank Greg O. Cron for editing the English text.

REFERENCES

1. Vaupel P, Kelleher DK, Thews OT. Modulation of tumor oxygenation. *Int. J. Radiat. Oncol. Biol. Phys.* 1998; **42**: 843–848.
2. Less JR, Shalak TC, Sevick EM, Jain RK. Microvascular architecture in a mammary carcinoma: branching patterns and vessel dimension. *Cancer Res.* 1991; **51**: 265–273.
3. Munn LL. Aberrant vascular architecture in tumors and its importance in drug-based therapies. *Drug Discov. Today* 2003; **8**: 396–403.
4. Hashizume H, Baluk P, Morikawa S, McLean JW, Thurston G, Roberge S, Jain RK, McDonald M. Openings between defective endothelial cells explain tumor vessel leakiness. *Am. J. Pathol.* 2000; **156**: 1363–1380.
5. McDonald DM, Baluk P. Significance of blood vessel leakiness in cancer. *Cancer Res.* 2002; **62**: 5381–5385.
6. Boucher Y, Leunig M, Jain RK. Tumor angiogenesis and interstitial hypertension. *Cancer Res.* 1996; **56**: 4264–4266.
7. Thomlinson RH, Gray LH. The histological structure of some human lung cancers and the possible implications for radiotherapy. *Br. J. Cancer* 1955; **9**: 539–549.
8. Vaupel P, Kallinowski F, Okunieff P. Blood flow, oxygen and nutrient supply, and metabolic environment of human tumors: a review. *Cancer Res.* 1989; **49**: 6449–6465.
9. Dewhirst MW, Ong ET, Braun RD, Smith B, Klitzman B, Evans SM, Wilson D. Quantification of longitudinal tissue pO_2 gradients in window chamber tumours: impact on tumour hypoxia. *Br. J. Cancer* 1999; **79**: 1717–1722.
10. Secomb TW, Hsu R, Braun RD, Ross JR, Gross JF, Dewhirst MW. Theoretical simulation of oxygen transport to tumors by three-dimensional networks of microvessels. *Adv. Exp. Med. Biol.* 1998; **454**: 629–634.
11. Dewhirst DW. Concepts of oxygen transport at the microcirculatory level. *Semin. Radiat. Oncol.* 1998; **8**: 143–150.
12. Chaplin DJ, Durand RE, Olive PL. Acute hypoxia in tumors: implications for modifiers of radiation effects. *Int. J. Radiat. Oncol. Biol. Phys.* 1986; **12**: 1279–1282.
13. Dewhirst MW, Kimura H, Rehmus SW, Braun RD, Papahadjopoulos D, Hong K, Secomb TW. Microvascular studies on the origins of perfusion-limited hypoxia. *Br. J. Cancer* 1996; **27**: S247–S251.
14. Trotter MJ, Olive PL, Chaplin DJ. Effect of vascular marker Hoechst 33342 on tumor perfusion and cardiovascular function in the mouse. *Br. J. Cancer* 1990; **62**: 903–908.
15. Chaplin DJ, Hill SA. Temporal heterogeneity in microregional erythrocyte flux in experimental solid tumors. *Br. J. Cancer* 1990; **62**: 903–908.
16. Hill SA, Pigott KH, Saunders MI, Powell ME, Arnold S, Obeid A, Ward G, Leahy M, Hoskin PJ, Chaplin DJ. Microregional blood flow in murine and human tumors assessed using laser-Doppler microprobes. *Br. J. Cancer* 1996; **27**: S260–S263.
17. Braun RD, Lanzen JL, Dewhirst MW. Fourier analysis of fluctuations of oxygen tension and blood flow in R3230Ac tumors and muscle in rats. *Am. J. Physiol.* 1999; **277**: H551–H568.

18. Kimura H, Braun RD, Ong ET, Hsu R, Secomb TW, Papahadjopoulos D, Hong K, Dewhirst MW. Fluctuations in red cell flux in tumor microvessels can lead to transient hypoxia and reoxygenation in tumor parenchyma. *Cancer Res.* 1996; **56**: 5522–5528.
19. Intaglietta M, Myers RR, Gross JF, Reinhold HS. Dynamics of microvascular flow in implanted mouse mammary tumors. *Bibl. Anat.* 1977; **15**: 273–276.
20. Patan S, Munn LL, Jain RK. Intususceptive microvascular growth in a human colon adenocarcinoma xenograft: a novel mechanism of tumor angiogenesis. *Microvasc. Res.* 1996; **51**: 260–272.
21. Kiani MF, Pries AR, Hsu LL, Sarelius IH, Cokelet GR. Fluctuations in microvascular blood flow parameters caused by hemodynamic mechanisms. *Am. J. Physiol.* 1994; **266**: H1822–H1828.
22. Mollica F, Jain RK, Netti PA. A model for temporal heterogeneities of tumor blood flow. *Microvasc. Res.* 2003; **65**: 56–60.
23. Rofstad EK. Micro-environment-induced cancer metastasis. *Int. J. Radiat. Biol.* 2000; **76**: 589–605.
24. Young SD, Marshall RS, Hill RP. Hypoxia induced DNA overreplication and enhances metastatic potential of murine tumor cels. *Proc. Natl Acad. Sci. USA* 1998; **85**: 9533–9537.
25. Rofstad EK, Danielsen T. Hypoxia induces metastasis of human melanoma cells: involvement of VEGF mediated angiogenesis. *Br. J. Cancer* 2002; **80**: 1697–1707.
26. Cairns RA, Kalliomaki T, Hill RP. Acute (cyclic) hypoxia enhances spontaneous metastasis of KHT murine tumors. *Cancer Res.* 2001; **61**: 8903–8908.
27. Graeber TG, Osmanian C, Jacks T, Housman DE, Koch CJ, Lowe SW, Giaccia AJ. Hypoxia mediated selection of cells with diminished apoptotic potential in solid tumors. *Nature* 1996; **379**: 88–91.
28. Hockel M, Schlenger K, Hockel S, Vaupel P. Hypoxic cervical cancers with low apoptotic index are highly aggressive. *Cancer Res.* 1999; **59**: 4525–4528.
29. Semenza GL. Regulation of hypoxia-induced angiogenesis: a chaperone escorts VEGF to the dance. *J. Clin. Invest.* 2001; **108**: 39–40.
30. Harris AL. Hypoxia: a key regulatory factor in tumor growth. *Nat. Rev. Cancer* 2002; **2**: 38–47.
31. Semenza GL. The metabolism of tumors: 70 years later. *Novartis Found. Sympos.* 2001; **240**: 251–260.
32. Hockel M, Vaupel P. Tumor hypoxia: definitions and current clinical, biologic and molecular aspects. *J. Natl Cancer Inst*. 2001; **93**: 266–276.
33. Hall EJ. *Radiobiology for the Radiologist*, 4th edn. Lippincott: Philadelphia, PA, 1994.
34. Gray LH, Conger AD, Ebert M, Hornsey S, Scott OC. The concentration of oxygen dissolved in tissues at the time of irradiation as a factor in radiotherapy. *Br. J. Radiol.* 1953; **26**: 638–648.
35. Hill RP. Cellular basis for radiotherapy. In *The Basic Science of Oncology*, 2nd edn, Tannock IF, Hill RP (eds). McGraw-Hill: New York, 1992; 259–275.
36. Gatenby RA, Kessler HB, Rosenblum JS, Coia LR, Broder PJ. Oxygen distribution in squamous cell carcinoma metastases and its relationship to outcome of radiation therapy. *Int. J. Radiat. Oncol. Biol. Phys.* 1987; **14**: 831–838.
37. Hockel M, Knoop C, Schlenger K, Baussman E, Mitze M, Knapstein P, Vaupel P. Intratumoral pO_2 predicts survival in advanced cancer of the uterine cervix. *Radiother. Oncol.* 1993; **26**: 45–50.
38. Hockel M, Knoop C, Schlenger K, Baussman E, Knapstein P. Tumor oxygenation: a new predictive parameter in locally advanced cancer of the cervix. *Gynecol. Oncol.* 1993; **51**: 141–149.
39. Hockel M, Schlenger K, Mitze M, Schaffer U, Vaupel P. Hypoxia and radiation response in human tumors. *Semin. Radiat. Oncol.* 1996; **6**: 3–9.
40. Okunieff P, Hoeckelm M, Dunphy EP, Schlenger K, Knoop C, Vaupel P. Oxygen tension distributions are sufficient to explain the local response of human breast tumors treated with radiation alone. *Int. J. Radiat. Oncol. Biol. Phys.* 1993; **26**: 631–636.
41. Stone HB, Brown JM, Philips TL, Sutherland RM. Oxygen in human tumors: correlation between methods of measurement and response to therapy. *Radiat. Res.* 1993; **136**: 422–434.
42. Thomas CD, Chavaudra N, Martin L, Guichard M. Correlation between radiosensitivity, percentage hypoxic cells and pO_2 measurements in one rodent and two human xenografts. *Radiat. Res.* 1994; **139**: 1–8.
43. Swartz HM. The measurement of oxygen *in vivo* using EPR techniques. In *in Vivo EPR (ESR): Theory and Applications: Biological Magnetic Resonance*, Vol. 18, Berliner LJ (ed.). Kluwer Academic/Plenum: New York, 2003; 403–440.
44. Durand RE. The influence of microenvironmental factors during cancer therapy. *In Vivo* 1994; **8**: 691–702.
45. Tannock IF. The relation between cell proliferation and the vascular system in a transplanted mammary tumor. *Br. J. Cancer* 1968; **22**: 258–273.
46. Olive PL. Distribution, oxygenation and clonogenicity of macrophages in a murine tumor. *Cancer Commun*. 1989; **1**: 93–100.
47. Teicher BA, Holden SA, Al-Achi A, Herman TS. Classification of anti-neoplastic treatments by their differential toxicity toward putative oxygenated and hypoxic tumor subpopulations *in vivo* in the FSaII murine fibrosarcoma. *Cancer Res.* 1990; **50**: 3339–3344.
48. Sakata K, Kwok TT, Murphy BJ, Laderoute KR, Gordon GR, Sutherland RM. Hypoxia-induced drug resistance: comparison to P-glycoprotein-associated drug resistance. *Br. J. Cancer* 1991; **64**: 809–814.
49. Anthoney DA, McIlwrath AJ, Gallagher WM, Edlin AR, Brown R. Microsatellite instability, apoptosis, and loss of p53 function in drug-resistant tumor cells. *Cancer Res.* 1996; **56**: 1374–1381.
50. Sethi T, Rintoul RC, Moore SM, MacKinnon AC, Salter D, Choo C, Chilvers ER, Dransfield I, Donnelly SC, Strieter R, Haslett C. Extracellular matrix proteins protect small cell lung cancer against apoptosis: a mechanism for small cell lung cancer growth and drug resistance *in vivo. Nat. Med.* 1999; **5**: 662–668.
51. Durand RE. Intermittent blood flow in solid tumors. An underappreciated source of drug resistance. *Cancer Metastasis Rev.* 2001; **20**: 57–61.
52. Durand RE. Clinical relevance of intermittent tumour blood flow. *Acta Oncol*. 2001; **40**: 929–936.
53. Kallinowski F, Zander R, Hoeckel M, Vaupel P. Tumor tissue oxygenation as evaluated by computerized-pO_2-histography. *Int. J. Radiat. Oncol. Biol. Phys.* 1990; **19**: 953–961.
54. Dewhirst MW, Klitzman B, Braun RD, Brizel DM, Haroon ZA, Secomb TW. Review of methods to study oxygen transport at the microcirculatory level. *Int. J. Cancer* 2000; **90**: 237–255.
55. Dewhirst MW, Secomb TW, Ong ET, Hsu R, Gross JF. Determination of local oxygen consumption rates in tumors. *Cancer Res.* 1994; **54**: 3333–3336.
56. Dewhirst MW, Ong ET, Rosner GL, Rehmus SW, Shan S, Brau RD, Brizel DM, Secomb TW. Arteriolar oxygenation in tumour and subcutaneous arterioles: effects of inspired air oxygen content. *Br. J. Cancer* 1996; **27**: S241–S246.
57. Lanzen JL, Braun RD, Ong AL, Dewhirst MW. Variability in blood flow and pO_2 in tumors in response to carbogen breathing. *Int. J. Radiat. Oncol. Biol. Phys*. 1998; **42**: 855–859.
58. Ressel A, Weiss C, Feyerabend T. Tumor oxygenation after radiotherapy, chemotherapy, and/or hyperthermia predicts tumor free survival. *Int. J. Radiat. Oncol. Biol. Phys.* 2001; **49**: 1119–1125.
59. Griffiths JR, Robinson SP. The OxyLite: a fiber optic oxygen sensor. *Br. J. Radiol*. 1999; **72**: 627–630.
60. Seddon BM, Honess DJ, Vojnovic B, Tozer GM, Workman P. Measurement of tumor oxygenation: *in vivo* comparison of a luminescence fiber-optic sensor and a polarographic electrode in the p22 tumor. *Radiat. Res.* 2001; **155**: 837–846.
61. Braun RD, Lanzen JL, Snyder SA, Dewhirst MW. Comparison of tumor and normal tissue oxygen tension measurements using OxyLite or microelectrode in rodents. *Am. J. Physiol.* 2001; **280**: H2533–H2544.
62. Bussink J, Kanders JH, Strik AM, vander Kogel AJ. Effects of nicotinamide and carbogen on oxygenation in human tumor xenografts measured with luminescence based fiber-optic probes. *Radiother. Oncol.* 2000; **57**: 21–30.
63. Demeure RJ, Jordan BF, Yang QX, Beghein N, Smith MB, Gregoire V, Gallez B. Removal of local field gradient artefacts

in BOLD contrast imaging of head and neck tumors. *Phys. Med. Biol.* 2002; **47**: 1819–1825.
64. Jarm T, Sersa G, Miklavcic D. Oxygenation and blood flow in tumors treated with hydralazine: evaluation with a novel luminescence-based fiber-optic sensor. *Technol. Health Care* 2002; **10**: 363–380.
65. Baudelet C, Gallez B. How does Blood Oxygen Level Dependent (BOLD) contrast correlate with oxygen partial pressure (pO_2) inside tumors? *Magn. Reson. Med.* 2002; **48**: 980–986.
66. Jordan BF, Gregoire V, Demeure RJ, Sonveaux P, Feron O, O'Hara JA, Vanhulle VP, Delzenne N, Gallez B. Insulin increases the sensitivity of tumors to irradiation: involvement of an increase in tumor oxygenation mediated by a nitric oxide-dependent decrease of the tumor cells oxygen consumption. *Cancer Res.* 2002; **62**: 3555–3561.
67. Jordan BF, Beghein N, Aubry M, Gregoire V, Gallez B. Potentiation of radiation-induced delay by isosorbide dinitrate in FSAII murine tumors. *Int. J. Cancer* 2003; **103**: 138–141.
68. Jordan BF, Sonveaux P, Feron O, Gregoire V, Beghein N, Gallez B. Nitric oxide mediated increase in tumor blood flow and oxygenation of tumors implanted in muscles stimulated by electric pulses. *Int. J. Radiat. Oncol. Biol. Phys.* 2003; **55**: 1066–1073.
69. Brurberg KG, Graff BA, Rofstad EK. Temporal heterogeneity in oxygen tension in human melanoma xenografts. *Br. J. Cancer* 2003; **21**: 350–356.
70. Wilson DF, Vinogradov SA, Dugan BW, Biruski D, Waldron L, Evans SA. Measurement of tumor oxygenation using new frequency domain phosphoremeters. *Comp. Biochem. Physiol. A Mol. Integr. Physiol.* 2002; **132**: 153–159.
71. Wilson DF. Oxygen dependent quenching of phosphorescence: a perspective. *Adv. Exp. Med. Biol.* 1992; **317**: 195–201.
72. Vinogradov SA, Lo LW, Jenkins WT, Evans SM, Koch C, Wilson DF. Non invasive imaging of the distribution in oxygen in tissue *in vivo* using near-infrared phosphors. *Biophys. J.* 1996; **70**: 1609–1617.
73. Hull EL, Conover DL, Foster TH. Carbogen-induced changes in rat mammary tumor oxygenation reported by near-infrared spectroscopy. *Br. J. Cancer* 1999; **79**: 1709–1716.
74. Liu HL, Song YL, Worden KL, Jiang X, Constantinescu A, Mason RP. Non invasive investigation of blood oxygenation dynamics of tumors by near-infrared spectroscopy. *Applied optics* 2000; **39**: 5231–5243.
75. Wray S, Cope M, Delpy DT, Wyatt JS, Reynolds OR. Characterisation of the near-infrared absorption spectra of cytochrome aa3 and haemoglobin for the non-invasive monitoring of cerebral oxygenation. *Biochim. Biophys. Acta* 1988; **933**: 184–192.
76. Varghese AJ, Gulyas S, Mohindra JK. Hypoxia-dependent reduction of 1-(2-nitro-1-imidazolyl)-3-methoxy-2-propanol by Chinese hamster ovary cells and KHT tumor cells *in vitro* and *in vivo. Cancer Res*. 1976; **36**: 3761–3765.
77. Raleigh JA, Franko AJ, Koch CJ, Born JL. Binding of misonidazole to hypoxic cells in monolayer and spheroid culture: evidence that a side-chain label is bound as efficiently as a ring label. *Br. J. Cancer* 1985; **51**: 229–235.
78. Raleigh JA, Koch CJ. Importance of thiols in the reductive binding of 2-nitroimidazoles to macromolecules. *Biochem. Pharmac*. 1990; **40**: 2457–2464.
79. Chapman JD, Franko AJ, Sharplin J. A marker for hypoxic cells in tumours with potential clinical applicability. *Br. J. Cancer* 1981; **43**: 546–550.
80. Gross MW, Karbach U, Groebe K, Franko AJ, Mueller-Klieser W. Calibration of misonidazole labeling by simultaneous measurement of oxygen tension and labeling density in multicellular spheroids. *Int. J. Cancer* 1995; **61**: 567–573.
81. Raleigh JA, Chou SC, Arteel GE, Horsman MR. Comparisons among pimonidazole binding, oxygen electrode measurements, and radiation response in C3H mouse tumors. *Radiat. Res.* 1999; **151**: 580–589.
82. Mahy P, De Bast M, Gallez B, Gueulette J, Koch CJ, Scalliet P, Grégoire V. *In vivo* co-localization of 2-nitroimidazole EF5 fluorescence intensity and electron paramagnetic resonance oximetry in mouse tumors. *Radiother. Oncol.* 2003; **67**: 53–61.
83. Josse O, Labar D, Georges B, Grégoire V, Marchand-Brynaert J. Synthesis of [^{18}F]-labeled EF3 [2-(2-nitroimidazol-1-yl)-N-(3,3,3-trifluoropropyl)-acetamide], a marker for PET detection of hypoxia. *Bioorg. Med. Chem.* 2001; **9**: 665–675.
84. Chapman JD, Engelhardt EL, Stobbe CC, Schneider RF, Hanks GE. Measuring hypoxia and predicting tumor radioresistance with nuclear medicine assays. *Radiother. Oncol.* 1998; **46**: 229–237.
85. Kennedy AS, Raleigh JA, Perez GM, Calkins DP, Thrall DE, Novotny DB, Varia MA. Proliferation and hypoxia in human squamous cell carcinoma of the cervix: first report of combined immunohistochemical assays. *Int. J. Radiat. Oncol. Biol. Phys.* 1997; **37**: 897–905.
86. Bussink J, Kaanders JH, Rijken PF, Peters JP, Hodgkiss RJ, Marres HA, van der Kogel AJ. Vascular architecture and microenvironmental parameters in human squamous cell carcinoma xenografts: effects of carbogen and nicotinamide. *Radiother. Oncol.* 1999; **50**: 173–184.
87. Gillies RJ, Raghunand N, Karczmar G, Bhujwalla ZM. MRI of the tumor microenvironment. *J. Magn. Reson. Imag.* 2002; **16**: 430–450.
88. Grucker D. Oxymetry by magnetic resonance: applications to animal biology and medicine. *Prog. Nucl. Magn. Reson. Spectrosc.* 2000; **36**: 241–270.
89. Ratner AV, Muller HH, Bradley-Simpson B, Johnson DE, Hurd RE, Sotak C, Young SW. Detection of tumors with ^{19}F magnetic resonance imaging. *Invest. Radiol.* 1988; **23**: 361–364.
90. Longmaid HE 3rd, Adams DF, Neirinckx RD, Harrison CG, Brunner P, Seltzer SE, Davis MA, Neuringer L, Geyer RP. *In vivo* ^{19}F NMR imaging of liver, tumor, and abscess in rats. Preliminary results. *Invest. Radiol.* 1985; **20**: 141–145.
91. Clark LC Jr, Ackerman JL, Thomas SR, Millard RW, Hoffman RE, Pratt RG, Ragle-Cole H, Kinsey RA, Janakiraman R. Perfluorinated organic liquids and emulsions as biocompatible NMR imaging agents for ^{19}F and dissolved oxygen. *Adv. Exp. Med. Biol.* 1984; **180**: 835–845.
92. Mason RP, Rodbumrung W, Antich PP. Hexafluorobenzene: a sensitive ^{19}F NMR indicator of tumor oxygenation. *NMR Biomed.* 1996; **9**: 125–134.
93. McIntyre DJO, McCoy CL, Griffiths JR. Tumour oxygenation measurements by F-19 magnetic resonance imaging of perfluorocarbons. *Curr. Sci.* 1999; **76**: 753–762.
94. Hunjan S, Zhao D, Constantinescu A, Hahn EW, Antich PP, Mason RP. Tumor oximetry: demonstration of an enhanced dynamic mapping procedure using fluorine-19 echo planar magnetic resonance imaging in the Dunning prostate R3327-AT1 rat tumor. *Int. J. Radiat. Oncol. Biol. Phys.* 2001; **49**: 1097–1108.
95. Mason RP, Ran S, Thorpe PE. Quantitative assessment of tumor oxygen dynamics: molecular imaging for prognostic radiology. *J. Cell. Biochem.* 2002; **39**(suppl.): 45–53.
96. Zhao D, Constantinescu A, Hahn EW, Mason RP. Differential oxygen dynamics in two diverse Dunning prostate R3327 rat tumor sublines (MAT-Lu and HI) with respect to growth and respiratory challenge. *Int. J. Radiat. Oncol. Biol. Phys.* 2002; **53**: 744–756.
97. Aboagye EO, Kelson AB, Tracy M, Workman P. Preclinical development and current status of the fluorinated 2-nitroimidazole hypoxia probe *N*-(2-hydroxy-3,3,3-trifluoropropyl)-2-(2-nitro-1-imidazolyl) acetamide (SR 4554, CRC 94/17): a non-invasive diagnostic probe for the measurement of tumor hypoxia by magnetic resonance spectroscopy and imaging, and by positron emission tomography. *Anticancer Drug Res.* 1998; **13**: 703–730.
98. Ogawa S, Lee TM, Kay AR, Tank DW. Brain magnetic resonance imaging with contrast dependent on blood oxygenation. *Proc. Natl Acad. Sci. USA* 1990; **87**: 9868–9872.
99. Ogawa S, Lee TM, Nayak AS, Glynn P. Oxygenation-sensitive contrast in magnetic resonance image of rodent brain at high magnetic fields. *Magn. Reson. Med.* 1990; **14**: 68–78.
100. Howe FA, Robinson SP, McIntyre DJ, Stubbs M, Griffiths JR. Issues in flow and oxygenation dependent contrast (FLOOD) imaging of tumours. *NMR Biomed.* 2001; **14**: 497–506.
101. Al-Hallaq HA, Fan X, Zamora M, River JN, Moulder JE, Karczmar GS. Spectrally inhomogeneous contrast changes detected in rodent tumors with high spectral and spatial resolution MRI. *NMR Biomed.* 2002; **15**: 28–36.

102. Kaanders JH, Bussink J, van der Kogel AJ. ARCON: a novel biology-based approach in radiotherapy. *Lancet Oncol.* 2002; **3**: 728–737.
103. Karczmar GS, Kuperman VY, River JN, Lewis MZ, Lipton MJ. Magnetic resonance measurement of response to hyperoxia differentiates tumors from normal tissue and may be sensitive to oxygen consumption. *Invest Radiol.* 1994; **29**: S161–S163.
104. Robinson SP, Howe FA, Griffiths JR. Noninvasive monitoring of carbogen-induced changes in tumor blood flow and oxygenation by functional magnetic resonance imaging. *Int. J. Radiat. Oncol. Biol. Phys.* 1995; **33**: 855–859.
105. Robinson SP, Rodrigues LM, Ojugo AS, McSheehy PM, Howe FA, Griffiths JR. The response to carbogen breathing in experimental tumour models monitored by gradient-recalled echo magnetic resonance imaging. *Br. J. Cancer* 1997; **75**: 1000–1006.
106. Griffiths JR, Taylor NJ, Howe FA, Saunders MI, Robinson SP, Hoskin PJ, Powell ME, Thoumine M, Caine LA, Baddeley H. The response of human tumors to carbogen breathing, monitored by gradient-recalled echo magnetic resonance imaging. *Int. J. Radiat. Oncol. Biol. Phys.* 1997; **39**: 697–701.
107. Jordan BF, Misson P, Demeure R, Baudelet C, Beghein N, Gallez B. Changes in tumor oxygenation/perfusion induced by the no donor, isosorbide dinitrate, in comparison with carbogen: monitoring by EPR and MRI. *Int. J. Radiat. Oncol. Biol. Phys.* 2000; **48**: 565–570.
108. Landuyt W, Hermans R, Bosmans H, Sunaert S, Beatse E, Farina D, Meijerink M, Zhang H, Van Den Bogaert W, Lambin P, Marchal G. BOLD contrast fMRI of whole rodent tumour during air or carbogen breathing using echo-planar imaging at 1.5 T. *Eur. J. Radiol.* 2001; **11**: 2332–2340.
109. Taylor NJ, Baddeley H, Goodchild KA, Powell ME, Thoumine M, Culver LA, Stirling JJ, Saunders MI, Hoskin PJ, Phillips H, Padhani AR, Griffiths JR. BOLD MRI of human tumor oxygenation during carbogen breathing. *J. Magn. Reson. Imag.* 2001; **14**: 156–163.
110. Rijpkema M, Kaanders JH, Joosten FB, van der Kogel AJ, Heerschap A. Effects of breathing a hyperoxic hypercapnic gas mixture on blood oxygenation and vascularity of head-and-neck tumors as measured by magnetic resonance imaging. *Int. J. Radiat. Oncol. Biol. Phys.* 2002; **53**: 1185–1191.
111. Robinson SP, Collingridge DR, Howe FA, Rodrigues LM, Chaplin DJ, Griffiths JR. Tumour response to hypercapnia and hyperoxia monitored by FLOOD magnetic resonance imaging. *NMR Biomed.* 1999; **12**: 98–106.
112. Howe FA, Robinson SP, Rodrigues LM, Griffiths JR. Flow and oxygenation dependent (FLOOD) contrast MR imaging to monitor the response of rat tumors to carbogen breathing. *Magn. Reson. Imag.* 1999; **17**: 1307–1318.
113. Lebon V, Carlier PG, Brillault-Salvat C, Leroy-Willig A. Simultaneous measurement of perfusion and oxygenation changes using a multiple gradient-echo sequence: application to human muscle study. *Magn. Reson. Imag.* 1998; **16**: 721–729.
114. Al-Hallaq HA, River JN, Zamora M, Oikawa H, Karczmar GS. Correlation of magnetic resonance and oxygen microelectrode measurements of carbogen-induced changes in tumor oxygenation. *Int. J. Radiat. Oncol. Biol. Phys.* 1998; **41**: 151–159.
115. Baudelet C, Gallez B. Cluster analysis of BOLD fMRI time series in tumors to study the heterogeneity of hemodynamic response to treatment. *Magn. Reson. Med.* 2003; **49**: 985–990.
116. Baudelet C, Ansiaux R, Jordan BF, Havaux X, Macq B, Gallez B. Physiological noise in murine solid tumors using T2* weighted gradient-echo imaging: a marker of tumor acute hypoxia? *Phys. Med. Biol.* 2004; **49**: 3389–3411.
117. Baudelet C, Anciaux R, Macq B, Gallez B. Non invasive mapping of spontaneous blood flow/oxygen fluctuations in tumors using functional Magnetic Resonance Imaging and their modifications by pharmacological treatments. *Proc. Int. Soc. Mag. Reson. Med.* 2003; **11**: 1225.
118. Mäder K, Stösser R, Borchert HH. Detection of free radicals in living mice after inhalation of DTBN by X-Band ESR. *Free Rad. Biol. Med.* 1993; **14**: 339–342.
119. Gallez B, Bacic G, Goda F, Jiang J, O'Hara JA, Dunn JF, Swartz HM. Use of nitroxides for assessing perfusion, oxygenation, and viability of tissues: *in vivo* EPR and MRI studies. *Magn. Reson. Med.* 1996; **35**: 97–106.
120. Nilges MJ, Walczak T, Swartz HM. 1 GHz *in vivo* ESR spectrometer operating with a surface probe. *Phys. Med.* 1989; **5**: 195–201.
121. Berliner LJ, Koscielniak J. Low-frequency EPR spectrometers: L band. In *EPR Imaging and in Vivo EPR*, Eaton GR, Eaton SS, Ohno K (eds). CRC Press: Boca Raton, FL, 1991; 65–77.
122. Halpern HJ, Bowman MK. Low frequency EPR spectrometers: MHz range. In *EPR Imaging and in Vivo EPR*, Eaton GR, Eaton SS, Ohno K (eds). CRC Press: Boca Raton, FL, 1991; 45–63.
123. Subramanian S, Mitchell JB, Krishna MC. Principles of *in vivo* EPR. In *in Vivo EPR (ESR): Theory and Applications: Biological Magnetic Resonance*, Vol. 18, Berliner LJ (ed.). Kluwer Academic/Plenum: New York, 2003; 23–40.
124. Krishna MC, Subramanian S, Kuppusamy P, Mitchell JB. Magnetic resonance imaging for *in vivo* assessment of tissue oxygenation concentration. *Semin. Radiat. Oncol.* 2001; **11**: 58–69.
125. Koscielniak J. CW EPR signal detection bridges. In *in Vivo EPR (ESR): Theory and Applications: Biological Magnetic Resonance*, Vol. 18, Berliner LJ (ed.). Kluwer Academic/Plenum: New York, 2003; 61–72.
126. Lurie DJ. Free radical imaging. *Br. J. Radiol.* 2001; **74**: 782–784.
127. Subramanian S, Murugesan R, Devasahayam N, Cook JA, Afeworki M, Pohida T, Tschudin RG, Mitchell JB, Krishna MC. High speed data acqusition system and receiver configurations for time-domain radiofrequency electron paramagnetic resonance spectroscopy and imaging. *J. Magn. Reson.* 1999; **137**: 379–388.
128. Subramanian S, Yamada KI, Irie A, Murugesan R, Cook JA, Devasahayam N, Van Dam GM, Mitchell JB, Krishna MC. Non invasive *in Vivo* oximetric imaging by radiofrequency FT EPR. *Magn. Reson. Med.* 2002; **47**: 1001–1008.
129. Subramanian S, Mitchell JB, Krishna MC. Time-domain radio frequency EPR imaging. In *in Vivo EPR (ESR): Theory and Applications: Biological Magnetic Resonance*, Vol. 18, Berliner LJ (ed.). Kluwer Academic/Plenum: New York, 2003; 153–197.
130. Gallez B, Mäder K, Swartz HM. Non invasive measurement of the pH inside the gut by using pH-sensitive nitroxides. An *in vivo* EPR study. *Magn. Reson. Med.* 1996; **36**: 694–697.
131. Mäder K, Gallez B, Liu KJ, Swartz HM. Non invasive *in vivo* characterization of release processes in biodegradable polymers by low-frequency electron parmagnetic resonance spectroscopy. *Biomaterials* 1996; **17**: 457–461.
132. Mäder K, Bacic G, Domb A, Elmalak O, Langer R, Swartz HM. Non invasive *in vivo* monitoring of drug release and polymer erosion from biodegradable polymers by EPR spectroscopy and NMR imging. *J. Pharm. Sci.* 1997; **86**: 126–134.
133. Halpern HJ, Chandramouli GV, Barth ED, Yu C, Peric M, Grdina DJ, Teicher BA. Diminished aqueous microviscosity of tumors in murine models measured with *in vivo* radiofrequency electron paramagnetic resonance. *Cancer Res.* 1999; **59**: 5836–5841.
134. Hyde JS, Subczynski WK. Spin-label oximetry. In *Spin Labeling: Theory and Applications: Biological Magnetic Resonance*, Vol. 8, Berliner LJ, Reuben J (eds). Plenum Press: New York, 1989; 399–425.
135. Swartz HM, Glockner JF. Measurement of oxygen by EPRI and EPRS. In *EPR Imaging and in Vivo EPR*, Eaton GR, Eaton SS, Ohno K (eds). CRC Press: Boca Raton, FL, 1991; 261–290.
136. Turek P, Moussavi M, Andre JJ. Magnetic properties of the lithium phthalocyanine PI-radical. Role of dioxygen. *Europhys. Lett.* 1989; **8**: 275–280.
137. Bensebaa F, Andre JJ. Effect of oxygen on phthalocyanine radicals—1: ESR study of lithium phthalocyanine spin species at different oxygen concentrations. *J. Phys. Chem.* 1992; **96**: 5739–5745.
138. Bensebaa F, Petit P, Andre JJ. The effect of oxygen on phthalocyanine radicals—2: comparative study of 2 lithium phthalocyanine powder derivatives by continuous and pulsed ESR. *Synth. Metals* 1992; **52**: 57–69.
139. Lewis IC, Singer LS. Electron spin resonance and the mechanism of carbonization. *Chem. Phys. Carbon* 1981; **17**: 1–88.

140. Clarkson RB, Odintsov BM, Ceroke PJ, Ardenkjaer-Larsen JH, Fruiamu M, Belford RL. Electron paramagnetic resonance and dynamic nuclear polarization of char suspensions: surface science and oximetry. *Phys. Med. Biol.* 1998; **43**: 1907–1920.
141. Atsarkin VA, Demidov VV, Vasneva GA, Dzheparov FS, Ceroke PJ, Odintsov BM, Clarkson RB. Mechanisms of oxygen response in carbon-based sensors. *J. Magn. Reson.* 2001; **149**: 85–89.
142. Swartz HM, Clarkson RB. The measurement of oxygen *in vivo* using EPR techniques. *Phys. Med. Biol.* 1998; **43**: 1957–1975.
143. Kocherginsky N, Swartz HM. Terminology, classification and distribution of the nitroxides in cells. In *Nitroxide Spin Labels: Reactions in Biology and Chemistry*, Kocherginsky N, Swartz HM (eds). CRC Press: Boca Raton, FL, 1995; 15–26.
144. Gallez B, Debuyst R, Demeure R, Dejehet F, Grandin C, Van Beers B, Taper H, Pringot J, Dumont P. Evaluation of a nitroxyl fatty acid as liver contrast agent for magnetic resonance imaging. *Magn. Reson. Med.* 1993; **30**: 592–599.
145. Gallez B, Lacour V, Demeure R, Debuyst R, Dejehet F, De Keyser JL, Dumont P. Spin labelled arabinogalactan as MRI contrast agent. *Magn. Reson. Imag.* 1994; **12**: 61–69.
146. Halpern HJ, Yu C, Peric M, Barth E, Grdina DJ, Teicher BA. Oxymetry deep in tissues with low-frequency electron paramagnetic resonance. *Proc. Natl Acad. Sci. USA* 1994; **91**: 13047–13051.
147. Liu KJ, Grinstaff MW, Jiang J, Suslick KS, Swartz HM, Wang W. *In vivo* measurement of oxygen concentration using sonochemically synthsized microspheres. *Biophys. J.* 1994; **67**: 896–901.
148. Grucker D, Guiberteau T, Eclancher B, Chambron J, Chiarelli R, Rassat A, Subra G, Gallez B. Dynamic nuclear polarization with nitroxides dissolved in biological fluids. *J. Magn. Reson. B* 1995; **106**: 101–109.
149. Guiberteau T, Grucker D. Dynamic nuclear polarization imaging in very low magnetic fields as a non invasive technique for oximetry. *J. Magn. Reson.* 1997; **124**: 263–266.
150. Chen K, Glockner JF, Morse PD, Swartz HM. Effects of oxygen on the metabolism of nitroxide spin labels in cells. *Biochemistry* 1989; **28**: 2496–2501.
151. Pals MA, Swartz HM. Oxygen dependent metabolism of potential magnetic resonance contrast agents. *Invest. Radiol.* 1987; **22**: 497–501.
152. Swartz HM. Use of nitroxides to measure redox metabolis in cells and tissues. *J. Chem. Soc., Faraday Trans. 1* 1987; **83**: 191.
153. Swartz HM, Chen K, Pals M, Sentjurc M, Morse PD. Hypoxia-sensitive NMR contrast agents. *Magn. Reson. Med.* 1986; **3**: 169.
154. Kuppusamy P, Li H, Ilangovan G, Cardounel AJ, Zweier JL, Yamada K, Krishna MC, Mitchell JB. Noninvasive imaging of tumor redox status and its modification by tissue glutathione levels. *Cancer Res.* 2002; **62**: 307–312.
155. Ilangovan G, Li H, Zweier JL, Krishna MC, Mitchell JB, Kuppusamy P. *In vivo* measurement of regional oxygenation and imaging of redox status in RIF-1 murine tumor: effect of carbogen-breathing. *Magn. Reson. Med.* 2002; **48**: 723–730.
156. Ardenkjaer-Larsen JH, Laursen I, Leunbach I, Ehnholm G, Wistrand LG, Peterson JS, Golman K. EPR and DNP properties of certain novel single electron contrast agents intended for oximetric image. *J. Magn. Reson.* 1998; **133**: 1–12.
157. Panagiotelis I, Nicholson I, Hutchison JMS. Electron spin relaxation time measurements using radiofrequency longitudinally detected ESR and application in oximetry. *J. Magn. Reson.* 2001; **149**: 74–84.
158. Yong L, Harbridge J, Quine RW, Rinard GA, Eaton SS, Eaton GR, Mailer C, Barth E, Halpern HJ. Electron spin relaxation of triarylmethyl radicals in fluid solution. *J. Magn. Reson.* 2001; **152**: 156–161.
159. Matsumoto KI, Chandrika B, Lohman JAB, Mitchell JB, Krishna MC, Subramanian S. Application of continuous-wave EPR spectral-spatial image reconstruction techniques for *in vivo* EPR oxymetry: comparison of projection reconstruction and constant-time modalities. *Magn. Reson. Med.* 2003; **50**: 865–874.
160. Elas M, Williams BB, Parasca A, Mailer C, Pelizzari CA, Lewis MA, River JN, Karczmar GS, Barth ED, Halpern HJ. Quantitative tumor oxymetric images from 4D electron paramagnetic resonance imaging (EPRI): methodology and comparison with blood oxygen level-dependent (BOLD) MRI. *Magn. Reson. Med.* 2003; **49**: 682–691.
161. Golman K, Petersson JS, Ardenkjaer-Larsen JH, Leunbach I, Wistrand LG, Ehnholm G, Liu K. Dynamic *in vivo* oximetry using Overhauser enhanced MR imaging. *J. Magn. Reson. Imaging* 2000; **12**: 929–938.
162. Li H, Deng Y, He G, Kuppusamy P, Lurie DJ, Zweier JL. Proton electron double resonance imaging of the *in vivo* distribution and clearance of a triaryl methyl radical in mice. *Magn. Reson. Med.* 2002; **48**: 530–534.
163. Krishna MC, English S, Yamada K, Yoo J, Murugesan R, Devasahayam N, Cook JA, Golman K, Ardenkjaer-Laersen JH, Subramanian S, Mitchell JB. Overhauser enhanced magnetic resonance imaging for tumor oximetry: co-registration of tumor anatomy and tissue oxygen concentration. *Proc. Natl Acad. Sci. USA* 2002; **99**: 2216–2221.
164. Reddy TJ, Iwama T, Halpern HJ, Rawal VH. General synthesis of persistent trityl radicals for EPR imaging of biological systems. *J. Org. Chem.* 2002; **67**: 4635–4639.
165. Swartz HM. Measuring real levels of oxygen *in vivo*: opportunities and challenges. *Biochem. Soc. Trans.* 2002; **30**: 248–252.
166. Dunn JF, Swartz HM. *In vivo* electron paramagnetic resonance oximetry with particulate materials. *Methods* 2003; **30**: 159–166.
167. Liu KJ, Gast P, Moussavi M, Norby SW, Vahidi N, Walczak T, Wu M, Swartz HM. Lithium phthalocyanine: a probe for electron paramagnetic resonance oximetry in viable biological systems. *Proc. Natl Acad. Sci. USA* 1993; **90**: 5438–5442.
168. Hou H, Grinberg OY, Taie S, Leichtweis S, Miyake M, Grinberg S, Xie H, Csete M, Swartz HM. Electron paramagnetic resonance assessment of brain tissue oxygen tension in anesthetized rats. *Anesth. Analg.* 2003; **96**: 1467–1472.
169. Dunn JF, O'Hara JA, Zaim-Wadghiri Y, Lei H, Meyerand ME, Grinberg OY, Hou H, Hoopes PJ, Demidenko E, Swartz HM. Changes in oxygenation of intracranial tumors with carbogen: a BOLD MRI and EPR oximetry study. *J. Magn. Reson. Imag.* 2002; **16**: 511–521.
170. Lei H, Grinberg O, Nwaigwe CI, Hou HG, Williams H, Swartz HM, Dunn JF. The effects of ketamine–xylazine anesthesia on cerebral blood flow and oxygenation observed using nuclear magnetic resonance perfusion imaging and electron paramagnetic resonance oximetry. *Brain Res.* 2001; **913**: 174–179.
171. Ilangovan G, Manivannan A, Li H, Yanagi H, Zweier JL, Kuppusamy P. A naphthalocyanine-based EPR probe for localized measurements of tissue oxygenation. *Free Rad. Biol. Med.* 2002; **32**: 139–147.
172. Vahidi N, Clarkson RB, Liu KJ, Norby SW, Swartz HM. *In vivo* and *in vitro* EPR oximetry with fusinite: a new coal-derived, particulate EPR probe. *Magn. Reson. Med.* 1994; **31**: 139–146.
173. Norby SW, Swartz HM, Clarkson RB. Electron and light microscopy studies on particulate EPR spin probes lithium phthalocyanine, fusinite and synthetic chars. *J. Microsc.* 1998; **192**: 172–185.
174. James PE, Grinberg OY, Goda F, Panz T, O'Hara JA, Swartz HM. Gloxy: an oxygen-sensitive coal for accurate measurement of low oxygen tensions in biological systems. *Magn. Reson. Med.* 1997; **38**: 48–58.
175. Jordan BF, Baudelet C, Gallez B. Carbon-centered radicals as oxygen sensors for *in vivo* electron paramagnetic resonance: screening for an optimal probe among commercially available charcoals. *MAGMA* 1998; **7**: 121–129.
176. Gallez B, Jordan BF, Baudelet C, Misson PD. Pharmacological modifications of the partial pressure of oxygen in murine tumors: evaluation using *in vivo* EPR oximetry. *Magn. Reson. Med.* 1999; **42**: 627–630.
177. Boyer SJ, Clarkson RB. Electron paramagnetic reonance studies of an active carbon: the influence of preparation procedure on the oxygen response of the linewidth. *Colloid Surface A* 1994; **82**: 217–224.
178. Clarkson RB, Ceroke P, Norby SW, Odintsov BM. Stable particulate paramagnetic materials as oxygen sensors in EPR oximetry. In *in Vivo EPR (ESR): Theory and Applications: Biological Magnetic Resonance*, Vol. 18, Berliner LJ (ed.). Kluwer Academic/Plenum: New York, 2003; 233–257.
179. He J, Beghein N, Clarkson RB, Swartz HM, Gallez B. Microencapsulation of carbon particles used as oxygen sensors in EPR oximetry to stabilize their responsiveness to oxygen *in vitro* and *in vivo*. *Phys. Med. Biol.* 2001; **46**: 3323–3329.

180. He J, Beghein N, Ceroke P, Clarkson RB, Swartz HM, Gallez B. Development of biocompatible oxygen-permeable films holding paramagnetic carbon particles: evaluation of their performance and stability in EPR oximetry. *Magn. Reson. Med*. 2001; **46**: 610–614.
181. Swartz HM, Liu KJ, Goda F, Walczak T. India ink: a potential clinically applicable EPR oximetry probe. *Magn. Reson. Med.* 1994; **31**: 229–232.
182. Goda F, Liu KJ, Walczak T, O'Hara JA, Jiang J, Swartz HM. *In vivo* oximetry using EPR and India ink. *Magn. Reson. Med.* 1995; **33**: 237–245.
183. Lan M, Beghein N, Charlier N, Gallez B. Carbon blacks as EPR sensors for localized measurements of tissue oxygenation. *Magn. Reson. Med.* 2004; **51**: 1272–1278.
184. Smirnov AI, Norby SW, Clarkson RB, Walczak T, Swartz HM. Simultaneous multi-site EPR spectroscopy *in vivo*. *Magn. Reson. Med*. 1993; **30**: 213–220.
185. Berliner LJ, Fujii H. Magnetic resonance imaging of biological specimens by electron paramagnetic resonance of nitroxide spin labels. *Science* 1985; **227**: 517–519.
186. Berliner LJ, Fujii H, Wan XM, Lukiewicz SJ. Feasibility study of imaging a living murine tumor by electron paramagnetic resonance. *Magn. Reson. Med.* 1987; **4**: 380–384.
187. Ohno K. ESR imaging: a deconvolution method for hyperfine patterns. *J. Magn. Reson.* 1982; **50**: 145–150.
188. Woods RK, Bacic GG, Lauterbur PC, Swartz HM. Three-dimensional electron spin resonance imaging. *J. Magn. Reson.* 1989; **84**: 247–254.
189. Colacicchi S, Ferrari M, Sotgiu A. *In vivo* electron paramagnetic resonance spectroscopy/imaging: first experiences, problems, and perspectives. *Int. J. Biochem.* 1992; **24**: 205–214.
190. Kuppusamy P, Chzhan M, Zweier JL. Principles of imaging. In *in Vivo EPR (ESR): Theory and Applications: Biological Magnetic Resonance*, Vol. 18, Berliner LJ (ed.). Kluwer Academic/Plenum: New York, 2003; 99–152.
191. Woods RK, Dobrucki JW, Glockner JD, Morse PD, Swartz HM. Spectral-spatial imaging as a method for non invasive biological oximetry. *J. Magn. Reson.* 1989; **85**: 50–59.
192. Woods RK, Hyslop WB, Swartz HM. Mapping oxygen concentrations with 4D electron spin resonance spectral-spatial imaging. *Phys. Med.* 1989; **2–4**: 121–137.
193. Kuppusamy P, Chzhan M, Vij K, Shtynbuk M, Lefer DJ, Gianella E, Zweier JL. Three-dimensional spectral-spatial EPR imaging of free radicals in the heart: a technique for imaging tissue metabolism and oxygenation. *Proc. Natl Acad. Sci. USA* 1994; **91**: 3388–3392.
194. He G, Shankar RA, Chzhan M, Samouilov A, Kuppusamy P, Zweier JL. Noninvasive measurement of anatomic structure and intrluminal oxygenation in the gastrointestinal tract of living mice with spatial and spectral EPR imaging. *Proc. Natl Acad. Sci. USA* 1999; **96**: 4586–4591.
195. Velan SS, Spencer RGS, Zweier JL, Kuppusamy P. Electron paramagnetic resonance oxygen mapping (EPROM): direct visualization of oxygen concentration in tissue. *Magn. Reson. Med.* 2000; **43**: 804–809.
196. Ellis SJ, Velayutham M, Velan SS, Petersen EF, Zweier JL, Kuppusamy P, Spencer RGS. EPR oxygen mapping (EPROM) of engineered cartilage grown in a hollow-fiber bioreactor. *Magn. Reson. Med.* 2001; **46**: 819–826.
197. Kuppusamy P, Shankar RA, Zweier JL. *In vivo* measurement of arterial and venous oxygenation in the rat using 3D spectral-spatial electron paramagnetic resonance imaging. *Phys. Med. Biol.* 1998; **43**: 1837–1844.
198. He G, Samouilov A, Kuppusamy P, Zweier JL. *In vivo* imaging of free radicals: applications from mouse to man. *Moll. Cell. Biochem*. 2002; **234–235**: 359–367.
199. Lurie DJ, Bussell DM, Bell LH, Mallard JR. Proton electron double resonance imaging of free radicals in large aqueous samples. *J. Magn. Reson.* 1988; **76**: 366–370.
200. Lurie DJ, Foster MA, Yeung D, Hutchison JMS. Design, construction and use of a large-sample field-cycled PEDRI imager. *Phys. Med. Biol.* 1998; **43**: 1877–1886.
201. Foster MA, Seimenis I, Lurie DJ. The application of PEDRI to the study of free radicals *in vivo. Phys. Med. Biol.* 1998; **43**: 1893–1897.
202. Grucker D. *In vivo* detection of injected free radicals by Overhauser effect imaging. *Magn. Reson. Med.* 1990; **14**: 140–147.
203. Lurie DJ. Proton-electron double-resonance imaging (PEDRI). In *in Vivo EPR (ESR): Theory and Applications: Biological Magnetic Resonance*, Vol. 18, Berliner LJ (ed.). Kluwer Academic/Plenum: New York, 2003; 547–578.
204. Lurie DJ, Hutchison JMS, Bell LH, Nicholson I, Bussel DM, Mallard JR. Field-cycled proton–electron double-resonance imaging of free radicals in large aqueous samples. *J. Magn. Reson.* 1989; **84**: 431–437.
205. Grucker D, Chambron J. Oxygen imaging in perfused hearts by dynamic nuclear polarization. *Magn. Reson. Imag.* 1993; **11**: 691–696.
206. Grucker D, Guiberteau T, Eclancher B. Oximetry by dynamic nuclear polarization. *Magn. Reson. Med*. 1995; **34**: 219–226.
207. Friedman BJ, Grinberg OY, Isaacs K, Walczak T, Swartz HM. Myocardial oxygen tension and relative capillary density in isolated perfused rat hearts. *J. Mol. Cell. Cardiol.* 1995; **27**: 2551–2558.
208. Friedman BJ, Grinberg OY, Isaacs K, Ruuge EK, Swartz HM. Effect of repetitive ischemia on local myocardial oxygen tension in isolated perfused and hypoperfused rat hearts. *Magn. Reson. Med.* 1996; **35**: 214–220.
209. Grinberg OY, Friedman BJ, Swartz HM. Intramyocardial pO_2 measured by EPR. *Adv. Exp. Med. Biol.* 1997; **428**: 261–268.
210. Zweier JL, Thompson-Gorman S, Kuppusamy P. Measurement of oxygen concentration in the intact beating heart using electron paramagnetic resonance spectroscopy: a technique for measuring oxygen concentration in situ. *J. Bioenerg. Biomembr.* 1991; **23**: 855–871.
211. Zweier JL, Samouilov A, Kuppusamy P. Cardiac applications of *in vivo* EPR spectroscopy and imaging. In *in Vivo EPR (ESR): Theory and Applications: Biological Magnetic Resonance*, Vol. 18, Berliner LJ (ed.). Kluwer Academic/Plenum: New York, 2003; 441–468.
212. Nakashima T, Goda F, Jiang J, Shima T, Swartz HM. Use of EPR oximetry with India ink to measure the pO_2 in the liver *in vivo* in mice. *Magn. Reson. Med.* 1995; **34**: 888–892.
213. Jiang J, Nakashima T, Shima T, Liu KJ, Goda F, Swartz HM. Measurement of pO_2 in liver using EPR oximetry. *J. Appl. Physiol.* 1996; **80**: 552–558.
214. Gallez B, Debuyst R, Dejehet F, Liu KJ, Walczak T, Goda F, Demeure R, Taper H, Swartz HM. Small particles of fusinite and carbohydrate chars coated with aqueous soluble polymers: preparation and applications for EPR oximetry. *Magn. Reson. Med.* 1998; **40**: 152–159.
215. James PE, Madhani M, Roebuck W, Jackson SK, Swartz HM. Endotoxin-induced liver hypoxia: defective oxygen delivery versus oxygen consumption. *Nitric Oxide* 2002; **6**: 18–28.
216. Madhani M, Barchowsky A, Klei L, Ross CR, Jackson SK, Swartz HM, James PE. Antibacterial peptide PR-39 affects local nitric oxide and preserves tissue oxygenation in the liver during septic shock. *Biochim. Biophys. Acta* 2002; **1588**: 232–240.
217. James PE, Miyake M, Swartz HM. Simultaneous measurement of NO and PO(2) from tissue by *in vivo* EPR. *Nitric Oxide* 1999; **3**: 292–301.
218. James PE, Bacic G, Grinberg OY, Goda F, Junn J, Jackson SK, Swartz HM. Endotoxin induced changes in intrarenal pO_2 measured by *in vivo* electron paramagnetic resonance oximetry and magnetic resonance imaging. *Free Rad. Biol. Med.* 1996; **21**: 25–34.
219. Krzic M, Sentjurc M, Kristl J. Improved skin oxygenation after benzoyl nicotinate application in different carriers as measured by EPR oximetry *in vivo. J. Control. Release* 2001; **70**: 203–211.
220. He G, Kutala VK, Kuppusamy P, Zweier JL. *In vivo* measurement and mapping of skin redox stress induced by ultraviolet light exposure. *Free Rad. Biol. Med.* 2004; **36**: 665–672.
221. Bacic G, Liu KJ, O'Hara JA, Harris RD, Szybinski K, Goda F, Swartz HM. Oxygen tension in a murine tumor: a combined EPR and MRI study. *Magn. Reson. Med.* 1993; **30**: 568–572.
222. Pandian RP, Parinandi NL, Ilangovan G, Zweier JL, Kuppusamy P. Novel particulate spin probe for targeted determination of oxygen in cells and tissues. *Free Rad. Biol. Med.* 2003; **35**: 1138–1148.
223. Goda F, O'Hara JA, Liu KJ, Rhodes ES, Dunn JF, Swartz HM. Comparisons of measurements of pO_2 in tissue *in vivo* by EPR

oximetry and microelectrodes. *Adv. Exp. Med. Biol.* 1997; **411**: 543–549.
224. Dunn JF, O'Hara JA, Zaim-Wadghiri Y, Lei H, Meyerand ME, Grinberg OY, Hou H, Hoopes PJ, Demidenko E, Swartz HM. Changes in oxygenation of intracranial tumors with carbogen: a BOLD MRI and EPR oximetry study. *J. Magn. Reson. Imag.* 2002; **16**: 511–521.
225. Song CW. Modification of blood flow. In *Blood Perfusion and Microenvironment of Human Tumors*, Molls M, Vaupel P (eds). Springer: Berlin, 1998; 193–207.
226. Wood PJ, Stratford IJ, Adams GE, Szabo C, Thiemermann C, Vane JR. Modification of the energy metabolism and radiation response of murine tumor by changes in nitric oxide availability. *Biochem. Biophys. Res. Commun.* 1993; **192**: 505–510.
227. Muruganandham M, Kasiviswanathan A, Jagannathan NR, Raghunathan P, Jain PC, Jain V. Diltiazem enhances tumor blood flow: MRI study in a murine tumor. *Int. J. Radiat. Oncol. Biol. Phys.* 1999; **43**: 416–421.
228. Jordan BF, Sonveaux P, Feron O, Grégoire V, Beghein N, Dessy C, and Gallez B. Nitric oxide as radiosensitizer: evidence for an intrinsic role additive to its effect on oxygen delivery and consumption. *Int. J. Cancer* 2004; **109**: 768–773.
229. Sersa G, Krzic M, Sentjurc M, Ivanusa T, Beravs K, Cemazar M, Auersperg M, Swartz HM. Reduced tumor oxygenation by treatment with vinbastine. *Cancer Res.* 2001; **61**: 4266–4271.
230. Sersa G, Krzic M, Sentjurc M, Ivanusa T, Beravs K, Kotnik V, Coer A, Swartz HM, Cemazar M. Reduced blood flow and oxygenation in SA-1 tumours after electrochemotherapy with cisplatin. *Br. J. Cancer* 2002; **87**: 1047–1054.
231. Goda F, O'Hara JA, Rhodes ES, Liu KJ, Dunn JF, Bacic G, Swartz HM. Changes of oxygen tension in experimental tumors after a single dose of X-ray irradiation. *Cancer Res.* 1995; **55**: 2249–2252.
232. O'Hara JA, Goda F, Liu KJ, Bacic G, Hoopes PJ, Swartz HM. The pO_2 in a murine tumor after irradiation: an *in vivo* electron paramagnetic resonance oximetry study. *Radiat. Res.* 1995; **144**: 222–229.
233. Goda F, Bacic G, O'Hara JA, Gallez B, Swartz HM, Dunn JF. The relationship between partial pressure of oxygen and perfusion in two murine tumors after X-ray irradiation: a combined gadopentetate dimeglumine dynamic magnetic resonance imaging and *in vivo* electron paramagnetic resonance oximetry study. *Cancer Res.* 1996; **56**: 3344–3349.
234. O'Hara JA, Goda F, Demidenko E, Swartz HM. Effect on regrowth delay in a murine tumor of scheduling split-dose irradiation based on direct pO_2 measurements by electron paramagnetic resonance oximetry. *Radiat. Res.* 1998; **150**: 549–556.
235. Sonveaux P, Dessy C, Brouet A, Jordan BF, Gregoire V, Gallez B, Balligand JL, Feron O. Modulation of the tumor vasculature functionality by ionizing radiation accounts for tumor radiosensitization and promotes gene delivery. *FASEB J.* 2002; **16**: 1979–1981.
236. Pogue BW, O'Hara JA, Demidenko E, Wilmot CM, Goodwin IA, Chen B, Swartz HM, Hasan T. Photodynamic therapy with verteporfin in the radiation-induced fibrosarcoma-1 tumor causes enhanced radiation sensitivity. *Cancer Res.* 2003; **63**: 1025–1033.
237. Pogue BW, O'Hara JA, Goodwin IA, Wilmot CJ, Fournier GP, Akay AR, Swartz H. Tumor PO(2) changes during photodynamic therapy depend upon photosensitizer type and time after injection. *Comp. Biochem. Physiol. A* 2002; **132**: 177–184.
238. O'Hara JA, Blumenthal RD, Grinberg OY, Demidenko E, Grinberg S, Wilmot CM, Taylor AM, Goldenberg DM, Swartz HM. Response to radioimmunotherapy correlates with tumor pO_2 measured by EPR oximetry in human tumor xenografts. *Radiat. Res.* 2001; **155**: 466–473.
239. Gordon DG, Brasch RC, Ogan MD, Deen D. Pyrroxamide, a nonionic nitroxyl spin label contrast agent for magnetic resonance imaging: mutagenesis and cell survival. *Invest Radiol*. 1988; **23**: 616–620.
240. Gallez B, De Meester C, Debuyst R, Dejehet F, Dumont P. Mutagenicity of nitroxyl compounds: structure-activity relationships. *Toxicol. Lett.* 1992; **63**: 35–45.
241. Sosnovsky G. A critical evaluation of the present status of toxicity of aminoxyl radicals. *J. Pharm. Sci*. 1992; **81**: 496–499.
242. Fuchs J, Groth N, Herrling T. Cutaneous tolerance to nitroxide free radicals in human skin. *Free Radic. Biol. Med.* 1998; **24**: 643–648.
243. Krishna MC, DeGraff W, Hankovszky OH, Sar CP, Kalai T, Jeko J, Russo A, Mitchell JB, Hideg K. Studies of structure-activity relationship of nitroxide free radicals and their precursors as modifiers against oxidative damage. *J. Med. Chem.* 1998; **41**: 3477–3492.
244. Gallez B, Mäder K. Accurate and sensitive measurements of pO_2 *in vivo* using low frequency EPR spectroscopy: how to confer biocompatibility to the oxygen sensors. *Free Rad. Biol. Med.* 2000; **29**: 1078–1084.
245. Gallez B, Jordan B, Baudelet C. Microencapsulation of paramagnetic particles by pyrroxylin in order to preserve their responsiveness to oxygen when used as sensors for *in vivo* EPR oximetry. *Magn. Reson. Med.* 1999; **42**: 193–196.
246. Gallez B, Debuyst R, Liu KJ, Demeure R, Dejehet F, Swartz HM. Development of biocompatible implants of fusinite for *in vivo* EPR oximetry. *MAGMA* 1996; **4**: 71–75.
247. Swartz HM. Potential medical (clinical) applications of EPR: overview and perspectives. In *in Vivo EPR (ESR): Theory and Applications: Biological Magnetic Resonance*, Vol. 18, Berliner LJ (ed.). Kluwer Academic/Plenum: New York, 2003; 599–621.
248. Lurie DJ, Foster MA, Yeung D, Hutchison JMS. Design, construction and use of a large-sample field-cycled PEDRI imager. *Phys. Med. Biol.* 1998; **43**: 1877–1886.
249. Lurie DJ, Li H, Petryakov S, Zweier JL. Development of a PEDRI free-radical imager using a 0.38 T clinical MRI system. *Magn. Reson. Med.* 2002; **47**: 181–186.

